Journal of Hazardous Materials 418 (2021) 126286

Contents lists available at ScienceDirect

Journal of Hazardous Materials

journal homepage: www.elsevier.com/locate/jhazmat

# β-cyclodextrin-containing polymer based on renewable cellulose resources for effective removal of ionic and non-ionic toxic organic pollutants from water

Koleta Hemine [a,*], Natalia Łukasik [a,*], Maria Gazda [b], Izabela Nowak [c]

[a] Department of Chemistry and Technology of Functional Materials, Faculty of Chemistry, Gdańsk University of Technology, 11/12 Narutowicza Street, 80-233 Gdańsk, Poland

[b] Institute of Nanotechnology and Materials Science, Faculty of Applied Physics and Mathematics, Gdańsk University of Technology, 11/12 Narutowicza Street, 80-233 Gdańsk, Poland

[c] Department of Applied Chemistry, Faculty of Chemistry, Adam Mickiewicz University, 8 Uniwersytetu Poznańskiego Street, 61-614 Poznań, Poland

ARTICLE INFO

Editor: Dr. H. Artuto

*Keywords:*
Cyclodextrin polymers
Adsorption
Toxic organic pollutants
Water treatment
Endocrine disrupting compound

ABSTRACT

A novel, bio-derived cyclodextrin-based trifunctional adsorbent has been successfully synthesized for efficient, rapid and simultaneous removal of a broad-spectrum of toxic ionic (anionic and cationic dyes) and non-ionic organic pollutants from water. The composition, morphology and the presence of functional groups in the obtained sorption material were characterized by elemental analysis, XRD, SEM, and FTIR spectroscopy. The adsorption results were represented by cationic dye (crystal violet, CV) and endocrine disrupting compound (bisphenol A, BPA) as an adsorbate. The sorption processes of the model pollutants were studied with both kinetic and equilibrium models. The results showed that the sorption was rapid (less than 1 min) and the time evolution could be fitted using a pseudo-second order model. According to Langmuir isotherm model, the maximum adsorption capacities were found at 113.64 and 43.10 mg $g^{-1}$ for BPA and CV, respectively. The adsorption ability of β-CDPs was kept nearly on the same level after five regeneration cycles. Furthermore, almost complete removal of the pollutants was observed during the treatment of real effluents samples thus the bio-derived, cheap and reusable BAN-EPI-CDP has a promising potential for practical applications.

## 1. Introduction

Wildlife and humans are permanently exposed to a variety of chemicals from different sources and via different routes, both in sequence and simultaneously (Kortenkamp and Faust, 2018). This leads to the presence of countless industrial and natural chemical compounds in the water cycle (Bernhardt et al., 2017; Schwarzenbach et al., 2006), which has now become one of the most important environmental problems. Textile industries are one of the most dye using and water-consuming economic sectors (Spagni et al., 2012). It is estimated that the amount of dyes used annually in the process of dyeing exceeds 50 billion-tons (Hu et al., 2020), of which ~20% are discharged into aqueous effluent (Huang et al., 2008; Yurtsever et al., 2015). Synthetic dyes usually have complex aromatic molecular structures and are often resistant toward oxidizing agents and biodegradation (Yadav et al., 2019). Dyes in the industrial effluents reduce water quality, as well as they are often toxic and potentially able to be transformed into teratogenic, carcinogenic, and mutagenic agents (Afkhami et al., 2010; Sansuk et al., 2016). In the dyeing process some auxiliaries with endocrine-disrupting effects, such as bisphenol A (BPA) derivatives are also present. BPA is a significant monomer in the formation of polycarbonates which can be used to the prevention of oxidation and degradation in textiles (Xue et al., 2017), and it has been detected in a majority of dye wastewater streams (Pothitou and Voutsa, 2008; Zhou et al., 2015). Endocrine disrupting chemicals (EDCs) even at very low concentration may cause an impact on hormonal control (Petrie et al., 2015; Zhou et al., 2019). In addition, these toxic compounds have complex chemical structures which cannot be naturally degraded in an easy way and removed from the environment (Gao et al., 2020). Commonly found water contamination such as aromatic micropollutants, dyes and EDCs represents a long-term potential risk to the ecosystem and living organisms (Alzate-Sánchez et al., 2019; Jia et al.,

* Corresponding authors.
*E-mail addresses:* koleta.hemine@pg.edu.pl (K. Hemine), natalia.lukasik@pg.edu.pl (N. Łukasik).

https://doi.org/10.1016/j.jhazmat.2021.126286
Received 20 March 2021; Received in revised form 29 May 2021; Accepted 30 May 2021
Available online 1 June 2021

2016; Yuan et al., 2020a). Therefore, it is urgent to treat this type of wastewater in a sustainable and economical way (Liu et al., 2020; Yuan et al., 2020a).

Several advanced approaches have been employed for the treatment of dyeing wastewater, such as oxidation processes (Cheng et al., 2004; Hassaan et al., 2017; Kos and Perkowski, 2003), biological degradation (Işik and Sponza, 2008; Jamee and Siddique, 2019; Yurtsever et al., 2015), coagulation/flocculation (Nabi Bidhendi et al., 2007; Verma et al., 2012; Zahrim and Hilal, 2013) and membrane filtration (Li et al., 2019; Thamaraiselvan and Noel, 2015). Nevertheless, these methods are not the best solution for industrial application due to their high operational cost, stringent environmental conditions, non-trivial operations, or their implementation may involve emission of more toxic by-products (Vakili et al., 2014). An example would be generation of organochlorine compounds from NaClO oxidation (Hu et al., 2020). Hu et al. (2002) described that during the chlorination disinfection, BPA could be transformed into various chlorinated by-products such as chlorine-BPA and dichloro-BPA, which have much higher estrogen-binding activity than BPA. In comparison to various types of water purification technologies, adsorption is inexpensive, fast, and characterized by easy operation and high efficiency without the generation of undesirable by-products (Ali and Gupta, 2007; Rosales et al., 2012). Currently, the most widely used adsorption agent in the industry is activated carbon with high levels of recovery of dyes. In spite of this, its use is limited by high cost, expensive regeneration and significantly decreased mass of adsorbent and adsorption efficiency after the recovery process (Bhatnagar and Minocha, 2006; Hu et al., 2020; Rosales et al., 2012; Sabio et al., 2004). Therefore, finding economic, non-conventional materials with high adsorption capacity before and after regeneration cycles is crucial for the practical applications for the advanced treating of dye wastewater.

Cyclodextrins (CDs) are cyclic oligosaccharides consisting of six (α-CD), seven (β-CD) or eight (γ-CD) glucose units, derived from enzymatic hydrolysis of starch (Crini, 2014; Szejtli, 1988). CDs can form inclusion complexes with specific compounds, which are a result of the size/shape match and the noncovalent bonding forces between CD hydrophobic cavity and guest molecules (Kozlowski and Sliwa, 2008; Szejtli, 1988; Szente and Szejtli, 2004). In recent years, these natural and non-toxic macrocyclic molecules (especially β-CD) attracted a lot of attention due to their characteristic hydrophobic cavity structure and the large numbers of modifiable hydroxyl (-OH) groups outside the macrocyclic rings (Zhou et al., 2018). These unique properties of β-CD make it an attractive and potentially feasible choice for the removal of various organic micro-pollutants from wastewater by means of adsorption (Huang et al., 2018). In comparison to commercial adsorbents, advantages of β-CD based adsorbents are: low cost, specific affinity and simple design (Wang et al., 2017). Due to the fact, that native CDs are soluble in water, they must be converted into water-insoluble materials using bifunctional linker, so that in such form they can be used for pollutant separation. Another approach is the CDs grafting onto insoluble support with high active surface such as zeolites (Mallard et al., 2015), cellulose (Qu et al., 2021b), silica gel (Shen et al., 2015), synthetic polymers (Guo et al., 2019; Zhou et al., 2018) or magnetic materials (Chen et al., 2019a; Liu et al., 2020). In comparison to materials composed only of CD units and a linker, sorbents obtained after CD immobilization may have higher sorption efficiency towards broader spectrum of pollutants as a solid support usually possess additional active sites. A solid support ensures also better mechanical strength, making this kind of sorbents attractive for potential industrial applications.

Under standard operating conditions, environmental pollution embraces a complex mixture of various contaminants, in different concentrations, from several sources. Practically, such a mixture is very hard to treat from wastewater (Liu et al., 2020), therefore it is important to develop systems able to remove selected pollutants from complex mixtures simultaneously. So far, reported cyclodextrin-based adsorbents for wastewater treatment have mainly limited adsorption capacity towards a single type of pollutant (Qin et al., 2019). The design of systems for multicomponent water purification with high efficiency still remains a challenge (Huang et al., 2018; Zhao et al., 2015; Zhou et al., 2018). In the development of such multifunctional sorbents a great role may play biomaterials derived from agricultural waste, which major advantages are low cost, availability, biodegradability, easiness in processing and regeneration. Among them banana peels are an interesting biosorbent (Akpomie and Conradie, 2020). The peels consisting of cellulose, hemicellulose, pectin and lignin were reported as effective materials for heavy metals (Afolabi et al., 2021) and dyes (Stavrinou et al., 2020) removal. In this work, a bio-derived, trifunctional cellulose-epichlorohydrin-β-cyclodextrin (BAN-EPI-CDP) adsorbent was successfully synthesized and characterized. The synthesis was carried out by the copolymerization reaction. Obtained a new, mesoporous β-CD based adsorbent with a high adsorption rate was used to remove simultaneously a broad-spectrum of toxic ionic (anionic and cationic dyes) and non-ionic organic pollutants (e.g. BPA) from water. For comparison reasons, difunctional EPI-CDP material was obtained. Analyzed pollutants are presented in Fig. S1, whereas model pollutants- crystal violet (CV) and bisphenol A (BPA) which were used to describe adsorption properties and isotherms are presented in Fig. 1. The mechanism of CV and BPA sorption by BAN-EPI-CDP was investigated, based on the interactions between pollutants, cellulose, cross-linker and native cyclodextrin. The use of a cheap, nontoxic and green material, which is cellulose derived from renewable raw materials (banana peels, which consists of 99% cellulose) (Ali, 2017) for the synthesis of cyclodextrin-based adsorbent has not been published so far. The small number of steps, low costs of production and reusability of the bio-derived sorbent cause that its obtainment is an environmentally friendly technology that can be easily incorporated on an industrial scale.

## 2. Experimental

### 2.1. Materials and methods

β-CD (98%) was purchased from Across Organic China/USA. Epichlorohydrin (EPI, ≥99%), bisphenol A (BPA, ≥99%), 2-naphthol (2-NP, 99%), 4-hydroxybiphenyl (4-HB, 97%), 4-nitroaniline (4-NA, ≥99%), diphenylamine (DPA, 99%), 2,4-dichlorophenol (2,4-DCP, 99%), chromotropic acid disodium salt (CA, ≥98%), crystal violet (CV, 96%), neutral red (NR, ≥90%), Congo red (CR, ≥97%), methylene blue

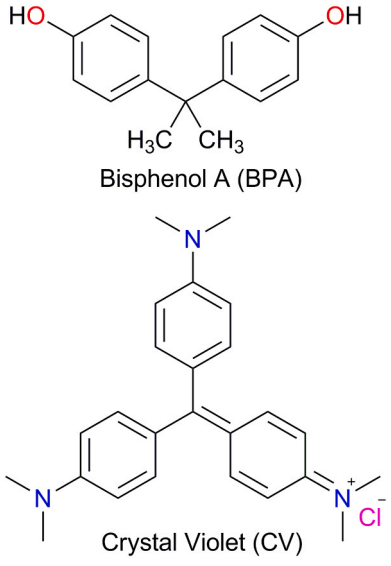


**Fig. 1.** Chemical formulas of model organic pollutants.

hydrate (MB, ≥95%), and phenosafranin (PhS, 80%) were supplied by Sigma–Aldrich, USA. Methanol ($CH_3OH$, ≥99.8%), ethanol ($C_2H_5OH$, anhydrous, ≥99.8%), nitric acid ($HNO_3$, 65%), sodium chloride (NaCl, analytical grade), sodium hydroxide (NaOH, analytical grade), potassium hydroxide (KOH, analytical grade) was purchased from POCH. Commercial humic acids containing 50% of humic acids and 50% of fulvic acids (HA, 90% dry matter) were supplied by Agraplant, Poland. Potassium bromide (KBr, spectroscopy grade) was purchased from Fisher Scientific and dried before use. All chemicals were used without further purification. Water used in all experiments was purified by Hydrolab-system (HLP- SPRING, temp. 22 °C, κ = 2.70 μS). Water from real water bodies was taken from the Orunski Park, Poland. Activated carbon Norit SX1 (N-SX1, $S_{BET}$ = 900 $m^2$) was obtained from Brenntag.

The raw material being a source of cellulose was dried in a muffle furnance Haraeus K114. The sorption materials were obtained with the use of an ultrasound bath Ultrasonic Cleaner KDC-2008, Getidy, and a rotary evaporator Büchi Rotavapor R-20. The final sorbents were prepared using a moisture analyzer (MA50 /1. R, Radwag) and a planetary ball mill (Pulverisette 7 classic line, Fritsch GmbH). Fourier transform infrared (FT-IR) spectra of the adsorbent (BAN, EPI-CDP, BAN-EPI-CDP) samples were recorded on a Thermo Nicolet iS10 using the KBr pellet method. The spectral resolution was 4 $cm^{-1}$ and the scanning range was from 400 to 4000 $cm^{-1}$. Powder X-ray diffraction (PXRD) measurements were investigated on a Philips X′Pert Pro diffractometer (Almelo, The Netherlands) with Cu Kα radiation. X-ray diffractograms were taken in the 2θ angle range of 5–70°. Nitrogen ($N_2$) adsorption- desorption isotherms were performed at −196 °C using a Micromeritics ASAP 2420 V2.09A apparatus. The specific surface area was measured by the Brunauer-Emmett-Teller (BET) (Brunauer et al., 1938) and Langmuir method. Pore size distribution (PSD) was measured using the classical Barrett-Joyner-Halenda (BJH) model (Barrett et al., 1951) and the Harkins and Jura t-Plot method. Scanning electron microscopy (SEM) observation was performed on a Quanta FEG 250 scanning electron microscope. Elemental analysis (EA) was obtained on a Flash 2000, Thermo Scientific CHN/O elemental analyzer. The UV-Vis spectrophotometric studies were performed using an UNICAM UV 300 spectrophotometer (an optical path 1 cm). In adsorption experiments a digital vortex mixer (OHAUS VXHDDG) and a MPW-250 centrifuge were applied.

### 2.2. Preparation of banana peels extract (BAN)

Bananas were purchased from a local market. Collected the raw waste banana peels were thoroughly washed with distilled water to remove surface impurities, cut into small pieces and dried in a muffle furnace for 24 h at 80 °C. The dried banana peels (BAN-P) were ground using a kitchen grinder. After that, 50 g of dried BAN-P were dispersed in 50 mL of 8 M KOH solution. Next, the suspension was treated with ultrasound for 1 h at the frequency of 40 KHz. Then, the suspension was soaked under air conditions for the next 24 h without stirring to ensure the full interactions between KOH and carbon sources in banana peels. Finally, the suspension was filtered, and dark brown filtrate- BAN, was collected for experimental uses.

To register FTIR spectra (Fig. S2) the alkaline BAN solution was neutralized by sulfuric acid. Then, the precipitate was washed several times with distilled water and dry.

### 2.3. Synthesis of BAN-EPI-CDP

β-CD (3.5 g) was dissolved in alkaline BAN solution (5.6 mL) and stirred at ambient temperature for 12 h. Next, EPI (3.5 mL) was slowly dripped to this solution with vigorous stirring at 30 °C. Polymerization was performed for 4 h. The reaction was stopped by the addition of acetone. The obtained precipitate was crushed with a spatula and then the solvent was evaporated under reduced pressure. The aqueous solution was neutralized by HCl 3 N and kept at 55 °C for 4 h. Then, the obtained precipitate was transferred to the falcon tube, where 40 mL of distilled water was added. The mixture was shaken for 5 min and centrifuged. The procedure was repeated three times. In the next step, the solid was washed three times with 50 mL of ethanol and dried in a moisture analyzer at 70 °C to a constant mass. Finally, the solid was homogenized by grinding in a planetary ball mill. A cream-colored fine powder was obtained (2.5 g) and subsequently characterized.

An analogous procedure was used for EPI-CDP synthesis. The detailed description can be found in Supplementary Information (SI, Text S1).

### 2.4. Determination of the β-CD content

The β-CD content of BAN-EPI-CDP and EPI-CDP was determined by spectrophotometric titration using phenolphthalein as the calibrant (Khalafi et al., 2016; Yuan et al., 2020a). To obtain a standard curve, the solutions of β-CD (0–0.34 mg $mL^{-1}$) were prepared in phenolphthalein solution (0.02 mg $mL^{-1}$, carbonate buffer solution pH 10.5). The samples were prepared by the addition of 1 mg of the sorption material (BAN-EPI-CDP or EPI-CDP) to 10 mL of phenolphthalein solution. The absorbance of these solutions was analyzed at 550 nm and compared with the standard curve. The β-CD substituent content (mmol $g^{-1}$) was calculated according to the equation:

$$\beta - CD \quad content = \frac{VC_{\beta-CD}}{mM_{\beta-CD}}, \tag{1}$$

where V (mL) is a sample solution volume, $C_{β\text{-}CD}$ is the concentration of β-CD (mg $mL^{-1}$) calculated on the basis of the standard curve, m (g) is the mass of the sorption material, and $M_{β\text{-}CD}$ is the molecular weight of β-CD (g $mol^{-1}$).

### 2.5. Water regain analysis

Experiments known as water regain of a material determine the change in mass before and after swelling. In this experiment, about 30 mg of BAN-EPI-CDP (BAN or EPI-CDP) was dispersed in deionised water for 18 h to reach the swelling equilibrium state. Then, the suspension was centrifuged at 13,000 rpm for 20 min. The supernatant was poured away, and the water on the surface of the sediment was reduced using a filter paper. After that, the sample was weighed. The water regain was calculated as follows:

$$Water \quad regain = \frac{w_w - w_d}{w_d} \cdot 100, \tag{2}$$

where, $w_w$ (mg) is the mass of the wet and $w_d$ (mg) of the dry adsorbent.

### 2.6. Adsorption experiments

All adsorption experiments were performed at 25 °C using BPA (68.5 mg $L^{-1}$) and CV (102.0 mg $L^{-1}$) aqueous solutions, however for experiments in binary system a mixture of BPA and CV (each at 0.15 mM) was used. In each analysis, an accurately weighed amount of the adsorbent was added to 5 mL of BPA or CV solution in plastic vials (7 mL) and sealed. Then, the mixture was shaken on a vortex mixer at 1000 rpm. Adsorption experiments were carried out for various time intervals and mass of adsorbent to resolve the adsorption equilibrium and maximum amount of BPA and CV adsorbed. Finally, aqueous suspensions were centrifuged at 13,000 rpm for 20 min and the BPA or CV concentrations in solutions were measured spectrophotometrically at the wavelength (λmax) of 276 and 590 nm, respectively. The efficiency of selected pollutant removal (%) was calculated using the following equation:

$$\text{Sorption efficiency} = \frac{C_0 - C_e}{C_0}, \tag{3}$$

where $C_0$ (mg $L^{-1}$) and $C_e$ (mg $L^{-1}$) are the initial and equilibrium concentration of BPA or CV in the stock solution and filtrate, respectively.

The amount of pollutant uptake was calculated based on the following equation:

$$q_e = \frac{(C_0 - C_e)V}{m}, \quad (4)$$

where $q_e$ (mg $g^{-1}$) is the amount of pollutant adsorbed per gram of sorbent, m (g) is the mass of the sorbent, V (L) is the volume of the aqueous pollutants solutions used.

### 2.7. Adsorption isotherms

The isothermal adsorption studies were performed using a batch equilibration technique, by adding 1 and 3 mg of adsorbent to 5 mL of a BPA and CV aqueous solutions, respectively. The stock solutions of BPA were set to be from 2.2 to 114.2 mg $L^{-1}$, while the initial concentration of CV was ranging from 7.4 to 300.7 mg $L^{-1}$. The mixtures were then shaken on a vortex mixer at 1000 rpm for 20 min to reach equilibrium. Finally, the suspensions were centrifuged. The absorbance of the supernatants of BPA and CV was measured spectrophotometrically at the wavelength of 276 and 590 nm, respectively.

The Freundlich, Langmuir and Sips equations were used to fit the adsorption isotherms.

The Freundlich isotherm is an empirical equation used to describe adsorption equilibrium on a heterogeneous surface, i.e., the adsorption sites are not energetically identical. The original form of the Freundlich equation can be given as follow (Ho et al., 2002):

$$q_e = K_F C_e^{1/n_F}, \quad (5)$$

where, $q_e$ (mg $g^{-1}$) is the equilibrium BPA or CV concentration on the adsorbent, $C_e$ (mg $g^{-1}$) is the adsorbate equilibrium concentration in the solution, $K_F$ ($L^{1/n}$ $mg^{1-1/n}$ $g^{-1}$) is the Freundlich constant and $1/n_F$ is the heterogeneity factor.

A linear form of the Freundlich adsorption isotherm calculated by plotting $\ln q_e$ versus $\ln C_e$ can be given as follows:

$$lnq_e = \frac{1}{n_F}\ln C_e + \ln K_F \quad (6)$$

The Langmuir model is based on the assumption of the adsorption of a monolayer on a homogeneous surface, the adsorption takes place at definite and localized sites and all the adsorption sites are energetically identical. The original form of the Langmuir equation is represented as follows (Ho et al., 2002):

$$q_e = \frac{K_L C_e}{1 + a_L C_e}, \quad (7)$$

where, $q_e$ (mg $g^{-1}$) is the equilibrium BPA or CV concentration on the adsorbent, $C_e$ (mg $L^{-1}$) is the adsorbate equilibrium concentration in the solution, $K_L$ (L $g^{-1}$) and $a_L$ (L $mg^{-1}$) are the Langmuir isotherm constants.

A linear form of the Langmuir adsorption isotherm was generated by plotting $C_e q_e^{-1}$ against $C_e$ in the following equation:

$$\frac{C_e}{q_e} = \frac{a_L}{K_L}C_e + \frac{1}{K_L} \quad (8)$$

The maximum adsorption capacity, $q_{max}$ of the adsorbent characterizing the theoretical monolayer capacity was determined as follows:

$$q_{max} = \frac{K_L}{a_L} \quad (9)$$

The equilibrium parameter, $R_L$, also called the separation factor, was calculated as follows (Hall et al., 1966; McKay, 2007):

$$R_L = \frac{1}{1 + a_L C_0}, \quad (10)$$

where, $C_0$ (mg $L^{-1}$) is the initial concentration of the adsorbate.

The $R_L$ value is based on the assumption of feasibility and the nature of the adsorption process. The value is specified in the following: irreversible ($R_L = 0$), favorable ($0 < R_L < 1$), linear ($R_L = 1$), unfavorable ($R_L > 1$).

Sips model consist of combination of Langmuir and Freundlich models. It is described by following equation:

$$q_e = \frac{q_{max} K_S C_e^{1/n_s}}{1 + K_s C_e^{1/n_s}} \quad (11)$$

where $K_s$ and $n_s$ are Sips equilibrium constant and exponent respectively (Lima et al., 2015).

### 2.8. Thermodynamic analysis

The thermodynamic parameters of adsorption process were determined using following equations:

$$\ln\left(K_e^0\right) = \frac{-\Delta H^0}{RT} + \frac{\Delta S^0}{R} \quad (12)$$

$$\Delta G^0 = -RT\ln(K_e^0) \quad (13)$$

$$K_e^0 = \frac{K M_{ad} c_{ad}^0}{\gamma} \quad (14)$$

where $\Delta G^0$, $\Delta H^0$, and $\Delta S^0$ are standard free energy, enthalpy, and entropy change respectively, $K_e^0$ is dimensionless thermodynamic equilibrium constant calculated using K (obtained from the best isotherm fitted, L $g^{-1}$), $M_{ad}$ is molecular weight of the adsorbate, $c_{ad}^0$ is standard concentration of the adsorbate (1 M) and $\gamma$ is the coefficient of activity (Lima et al., 2019).

### 2.9. Adsorption kinetics

Adsorption kinetic studies of BPA and CV were performed similarly as in described above adsorption experiments using 30 mg of BAN-EPI-CDP per each sample. To investigate kinetic behavior of the adsorbates linear pseudo-first (Lagergren, 1898) and pseudo-second (Ho and McKay, 1998) order models were applied (Eqs. 15 and 16 respectively):

$$\ln(q_e - q_t) = \ln q_e - k_1 t \quad (15)$$

$$\frac{t}{q_t} = \frac{1}{k_2 q_e^2} + \frac{t}{q_e}, \quad (16)$$

where $q_e$ and $q_t$ (mg $g^{-1}$) are adsorption uptakes at equilibrium and at time t (min), and $k_1$ (1/min) and $k_2$ (g $mg^{-1}$ $min^{-1}$) are the rate constants of pseudo-first and pseudo-second order, respectively.

Additionally, the intraparticle diffusion and Avrami fractional-order models, expressed by the following equations, were examined:

$$q_t = k_i t^{1/2} + C, \quad (17)$$

$$q_t = q_e\left(1 - e^{-(k_{Av}t)^n}\right), \quad (18)$$

where $q_t$ (mg $g^{-1}$) is the amount of the solute on the surface of the sorbate at time t, $k_i$ (mg $g^{-1}$ $min^{-0.5}$) is the intraparticle diffusion rate constant, and C is intercept (mg $g^{-1}$) (Weber and Morris, 1963), $k_{Av}$ is Avrami kinetic constant ($min^{-1}$), and n is Avrami exponent, which reflects mechanism changes that may take place during adsorption process (Qu et al., 2021a).

### 2.10. Effects of pH, humic acid and ionic strength

A BPA (5 mL, 68.5 mg $L^{-1}$) and CV (5 mL, 102.0 mg $L^{-1}$) solutions with specific pH level, ionic strength, and humic acid concentration were shaken for 20 min on a digital vortex mixer with 10 and 30 mg of the adsorbent, respectively. After that, aqueous suspensions were centrifuged at 13,000 rpm for 20 min and the BPA or CV concentrations in solutions were measured spectrophotometrically at the wavelength (λmax) of 276 and 590 nm, respectively. pH of aqueous solutions containing nitric acid or sodium hydroxide was determined with the use of a CPC-511 pH-meter combined with glass electrode (Elmetron, Poland). The humic acid concentration was set to 0–20 mg $L^{-1}$ and ionic strength represented by the concentration of NaCl was set to 0–3 M.

### 2.11. Regeneration experiments

0.01 g and 0.03 g of BAN-EPI-CDP was weighed and transferred to a 7 mL plastic vial, and 5 mL BPA (68.5 mg $L^{-1}$) and CV (102.0 mg $L^{-1}$) stock solution was added, respectively. Adsorbents regeneration studies were carried out by shaking of the suspensions on a digital vortex mixer at 25 °C for 20 min. After that, the mixtures were centrifuged at 13,000 rpm for 20 min and the BPA or CV concentrations in solutions were determined spectrophotometrically at the wavelength ($\lambda_{max}$) of 276 and 590 nm, respectively.

The BAN-EPI-CDP with adsorbed BPA, after the supernatant had been poured away, was regenerated by soaking sorbent in methanol (5 mL) and shaken it for 20 min. Finally, the BAN-EPI-CDP was recovered by centrifugation for 20 min at 13,000 rpm and used for the next experiments of the adsorption. The adsorption-desorption cycle was carried out five times.

The BAN-EPI-CDP with adsorbed CV, after the supernatant had been poured away, was regenerated by soaking sorbent in methanol (5 mL) and shaking it for 20 min. After that, BAN-EPI-CDP was recovered by centrifugation for 10 min at 13,000 rpm. This procedure was repeated 15 times till the content of CV in the supernatant measured spectrophotometrically was below the detection limit. After that, the sorbent was soaked in NaOH (0.01 M) and shaken for 40 min. Then, the mixture was centrifuged at 13,000 rpm for 20 min and supernatant was poured away. Next, the procedure was repeated. Then the sorbent was soaked in water till the moment of neutral pH of the supernatant, and next in methanol to remove water from the BAN-EPI-CDP. The adsorbent after regeneration was used for subsequent adsorption experiments. The adsorption-desorption cycle was carried out five times.

### 2.12. Environmental applications

The possibility of removing BPA and CV through the use of a BAN-EPI-CDP in real environmental conditions was evaluated by previous contamination with a known concentration of pollutants of natural water samples taken from the Oruński Park. The adsorption procedure was the same as for the model water samples. The 5 mL of BPA (68.5 mg $L^{-1}$) and CV (102.0 mg $L^{-1}$) in real water solutions was added to 10 mg and 30 mg of the adsorbent placed in plastic vials, respectively. The vials were sealed and the mixture was shaken on a digital vortex mixer at 1000 rpm for 20 min at 25 °C. After that, suspensions were centrifuged at 13,000 rpm for 20 min and the BPA or CV concentrations in solutions were measured spectrophotometrically.

### 2.13. Adsorption experiments of ionic and non-ionic pollutants through different type of adsorbents

The studies were carried out to compare the sorption efficiency of various ionic and nonionic impurities by different types of adsorbents: BAN, EPI-CDP, BAN-EPI-CDP. Ionic: CV, NR, CR, MB, PhS (5 mL, 0.05 mM) and non-ionic: BPA, 2-NP, 4-HB, 4-NA, DPA, 2,4-DCP (5 mL, 0.5 mM) aqueous solutions were shaken for 20 min on a digital vortex mixer with 30 mg of the BAN, EPI-CDP or BAN-EPI-CDP. Next, aqueous suspensions were centrifuged at 13,000 rpm for 20 min and the CV, NR, CR, MB, PhS, CA, BPA, 2-NP, 4-HB, 4-NA, DPA or 2,4-DCP concentrations in solutions were measured spectrophotometrically at the wavelength ($\lambda_{max}$) of 590, 532, 498, 665, 547, 347, 276, 328, 259, 411, 280, 285 nm, respectively.

### 2.14. Removal of pollutants from a complex mixture by the BAN-EPI-CDP

The BAN-EPI-CDP was used to remove the mixture of complex pollutants prepared in the laboratory. In the first step, 40 mL of an aqueous solution of ionic: CV, MB, NR, CA and non-ionic: 2-NP, BPA and 4-HB substances at a concentration of 0.3 mM in a plastic falcon tube (50 mL) was prepared. Then 250 mg of adsorbent was added and sealed. The mixture was then shaken on a vortex mixer at 1000 rpm. Finally, aqueous suspensions were centrifuged at 13,000 rpm for 20 min and each of the analyzed concentrations of pollutants in the solution was measured spectrophotometrically.

## 3. Results and discussion

### 3.1. Material design and characterization

The BAN-EPI-CDP polymer was prepared by crosslinking β-CD and cellulose raw material with EPI in alkaline solution (Scheme 1). In order to evaluate the β-CD content in obtained materials a spectrophotometric method was used (Khalafi et al., 2016; Yuan et al., 2020b). On the basis of a set of experiments with phenolphthalein it was determined that β-CD content in BAN-EPI-CDP and EPI-CDP was 4.71 and 4.74 mmol $g^{-1}$ respectively, which means that in both materials the content of β-CD is around 53% (Fig. S3). To prove that the change of the absorbance of phenolphthalein solution is an effect of the inclusion complex formation rather than simple adsorption into pores of a sorption material, experiments with banana peels were also carried out. For this material no changes in UV-Vis spectrum of phenolphthalein solution was observed. On the basis of the above and the results obtained from elemental analysis (Table S1) it was estimated that the content of epichlorohydrin-derived cross-linker (EPI) and cellulose obtained from banana peels (BAN-P) in BAN-EPI-CDP is 20.32% and 26.26%, respectively.

Surface functional groups of materials were detected by Fourier transform infrared spectrometry (FTIR). The FTIR spectra of the BAN-EPI-CDP, EPI-CDP and the raw materials (β-CD and BAN-P) were presented in Fig. 2a. The absorption bands of β-CD and BAN-P were in similar regions, because both materials have the same functional groups. As can be clearly seen from Fig. 2a, BAN-EPI-CDP has the same infrared absorption bands around 3423 $cm^{-1}$, 1637 $cm^{-1}$, 1400–1200 $cm^{-1}$ as β-CD and BAN-P which were attributed to hydroxyl –OH stretching vibration, H-O-H deformation bending of water molecules and C-H deformation vibrations bands in the primary and secondary hydroxyl groups. Additionally, the EPI molecules introduction during synthesis process is evidenced, because the band corresponding to the C-H stretching vibration at 2926 $cm^{-1}$ was broadened, and the band corresponding to the C-O-C stretching vibration at 1158 $cm^{-1}$ overlapped the band corresponding to the C-OH stretching vibration at 1029 $cm^{-1}$ related to the CD monomers. Similar influence of the EPI molecule presence on the FTIR spectrum was observed for EPI-CD material. The presence of characteristics functional groups of CD and BAN-P raw materials suggested that their structural units were essentially maintained in the polymers. Thus, FTIR results confirm that the syntheses of EPI-CDP and BAN-EPI-CDP were successfully carried out.

XRD was performed to examine the crystal structures of the samples (Fig. 2b). The BAN-P raw material presented one wide reflection at the 2θ of 21.8° which are characteristic of an amorphous structure. Due to the fact, that BAN-P are rich in potassium, seen in the diffractogram two

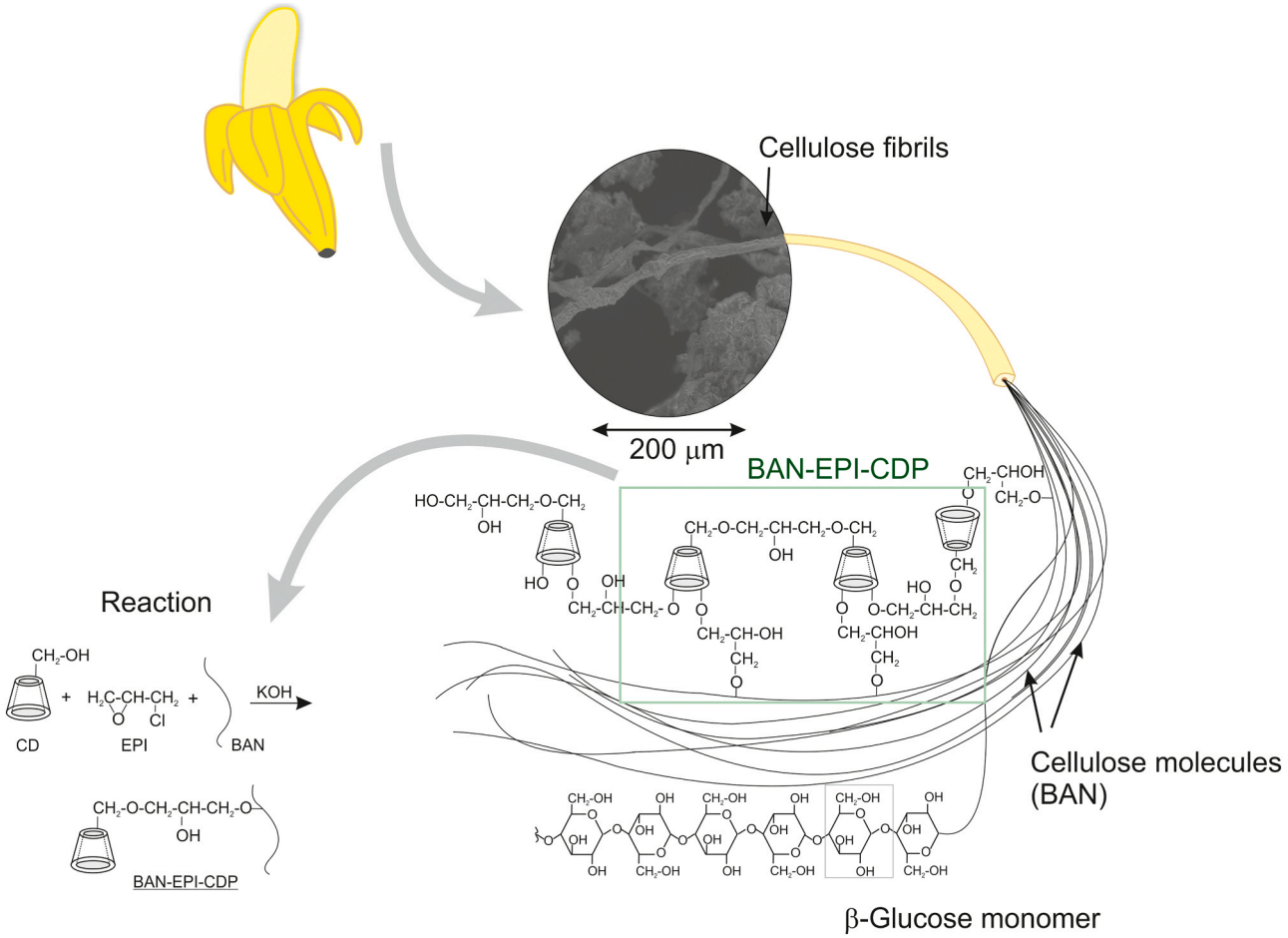


**Scheme 1.** Schematic chemical reaction between β-CD, EPI and BAN in an alkaline medium (left) and the proposed structure of BAN-EPI-CDP (right).

reflections (caption (♣)) at the 2θ of 28.3° and 40.6° can be attributed to a certain amount of potassium chloride present in the material. In contrast, sharp and intense reflections, the strongest of which at diffraction angles (2θ): 9.0°, 12.6°, 17.1°, 27.1° were observed in the XRD powder pattern for β-CD (caption (◆)), that confirmed its crystal structure nature. Importantly, the wide hump centered at the diffraction angle (2θ) about at 18.9° observed in EPI-CDP and BAN-EPI-CDP indicates that they were amorphous. The loss of crystallinity of these materials, was not related to the grinding process as it was confirmed by XRD pattern obtained before homogenization (Fig. S4). The amorphous character of EPI-CDP and BAN-EPI-CDP related to the loss of crystallinity of CD raw material during cross-linking reaction is an additional advantage as it promotes the sorption of target compounds [55].

The morphology of BAN-EPI-CDP sorbent was observed by SEM technique. As shown in Fig. 2c, the surface of the obtained sorbent appears to be dense and homogeneous with a small fraction of larger particles. The particle of BAN-EPI-CDP appeared to be irregular and shapeless. Interestingly, as can be seen in Fig. 2d, the BAN-EPI-CDP surface before the grinding process contains, besides particles of irregular shapes, the characteristic fibers that can be attributed to the cellulose fibers isolated from banana peels (Pelissari et al., 2014).

The water regain analysis, which determines the change in mass of the adsorbents before and after swelling, showed that the amounts of water that adsorbents could take up were 607%, 335% and 244% of their own weight, for BAN-P, EPI-CDP and BAN-EPI-CDP, respectively (Table S2). The obtained results indicated that, in contrast to BAN-P and EPI-CDP materials, BAN-EPI-CDP was characterized by the rigid structure (Xu et al., 2019).

The results of specific surface area and pore size distribution of BAN-EPI-CDP were presented in SI (Table S2, Text S2). As shown in Table S3, the BET and Langmuir surface areas for BAN-EPI-CDP were calculated to be approximately 2.29 and 3.28 $m^2\ g^{-1}$, respectively. The obtained results of the low values of both surface areas indicate that the surface chemical property, rather that the porous structure, was responsible for the adsorption of pollutants by BAN-EPI-CDP. Dried BAN-EPI-CDP was of the porous nature with average pore size at 21.3 nm and cumulative volume of pores at 0.009 $cm^3\ g^{-1}$ (Table S2). The Harkins and Jura t-Plot measurements (Fig. S6, Table S5) show that BAN-EPI-CDP does not contain micropores in its structure. The BAN-EPI-CDP showed the nature of mesoporous sorbent with pore size range of 2–50 nm (Fig. S7), which were in accordance with cyclodextrin-based polymer materials reported in literature (Liu et al., 2011).

### 3.2. Adsorption studies

#### 3.2.1. Effect of the adsorbent mass

The adsorption of electrically neutral BPA and cationic dye – CV was studied by changing of the sorbent quantity in the test solution maintaining the initial adsorbates concentration. The results presented in Fig. 3a shown that the percentage of removal increased with the adsorbent dosage in the case of both model pollutants. It can be attributed to the increased adsorbent surface, where more sorption sites are available. An equilibrium for BPA sorption was reached at a smaller amount of the adsorbent, i.e. 10 mg than for CV experiments, where 30 mg of the sorption material was needed to obtain maximum sorption efficiency. When 50 mg of BAN-EPI-CDP was used the percentage of BPA removal slightly decreased, what can be connected with overlapping or aggregation of adsorption sites. As a consequence the total surface area

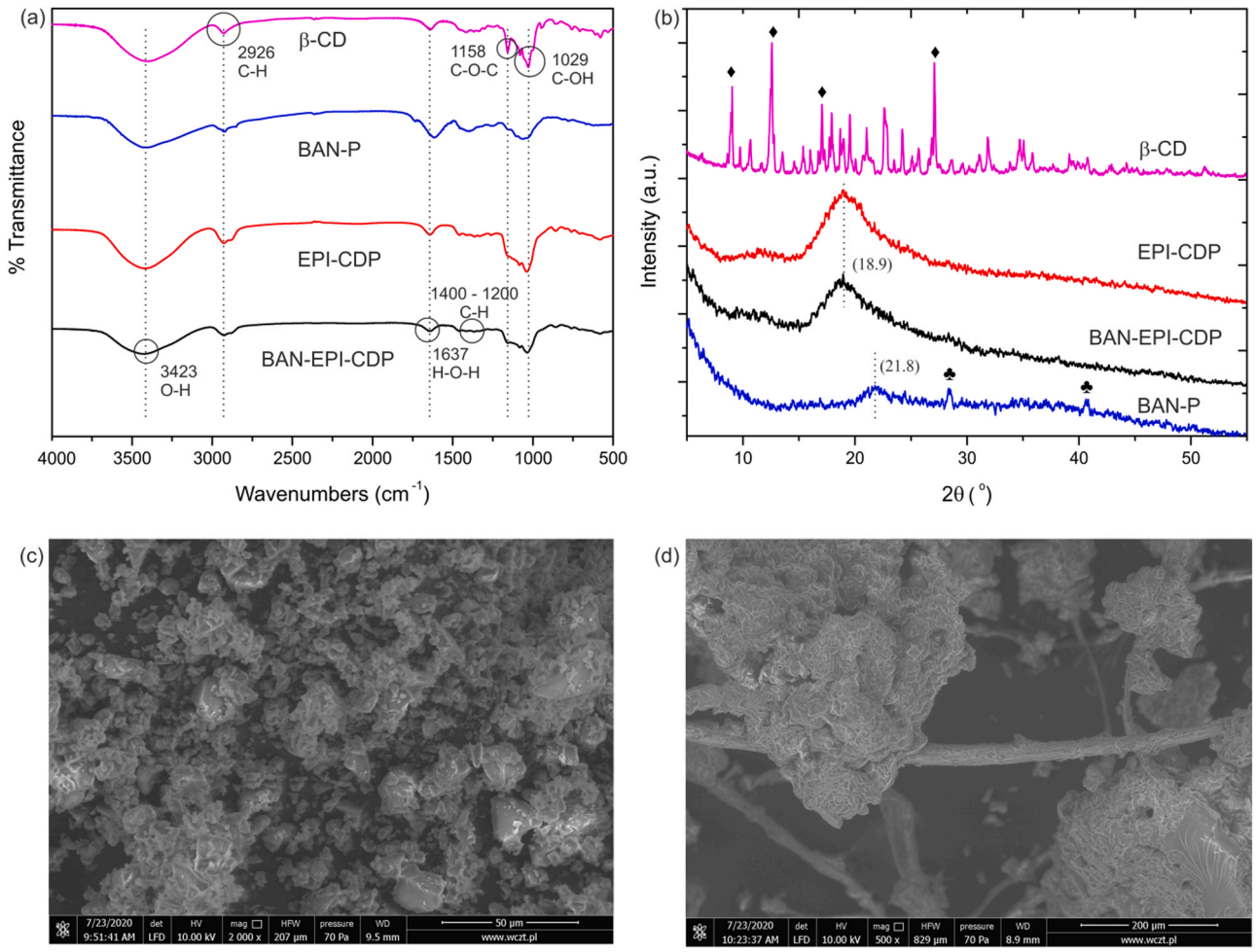


**Fig. 2.** (a) FTIR spectra, (b) XRD patterns of β-CD, BAN-P, EPI-CDP and BAN-EPI-CDP and SEM photographs of BAN-EPI-CDP material (c) after (mag 2000 x) and (d) before (mag 500 x) grinding process. Diffraction angles (2θ) from left for ◆: 9.0°, 12.6°, 17.1°, 27.1°, and for ♣: 28.3° and 40.6°.

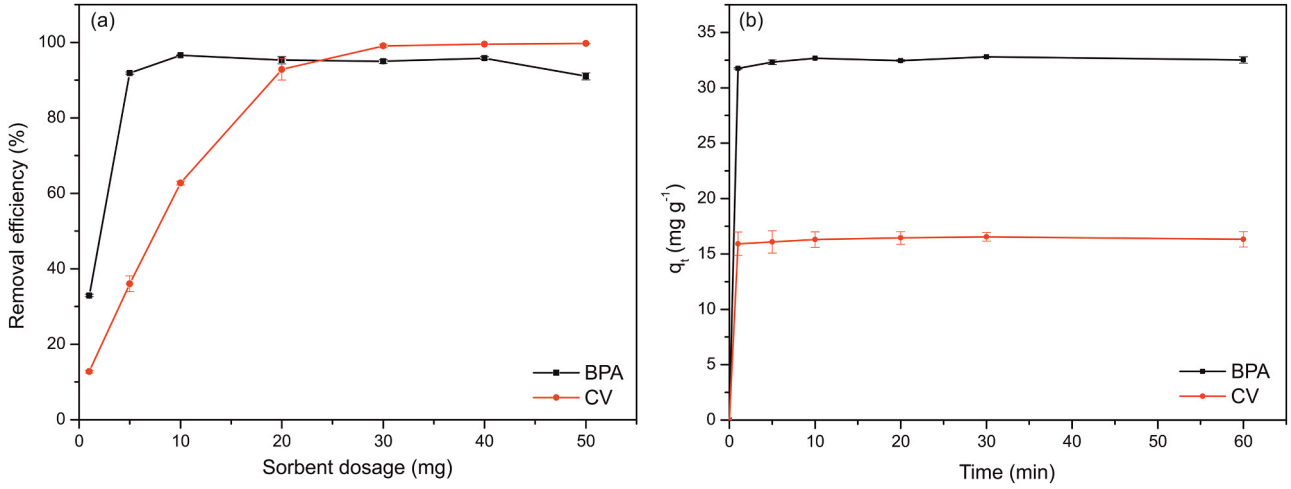


**Fig. 3.** Effect of (a) sorbent mass ($t_{contact}$ =20 min) and (b) time on adsorption of BPA (c = 68.5 mg $L^{-1}$, $m_{sor}$ = 10 mg) and CV (c = 102.0 mg $L^{-1}$, $m_{sor}$ = 30 mg) by BAN-EPI-CDP.

available for the pollutant decreases and the diffusion path length increases (Crini et al., 2007). Thus for the next experiments, 10 and 30 mg of the material for tests with BPA and CV respectively, were used. Similar tests carried out with the use of activated carbon shown that 10 and 5 mg of the material is sufficient for effective BPA and CV removal, respectively (Fig. S8). In a binary system removal of BPA by 10 mg of BAN-EPI-CDP slightly decreased, whereas it was more efficient for CV in comparison to single-component solutions (Fig. S9). Marginally lower adsorption efficiency in regard to BPA might be a consequence of competitive actions between the pollutants for active sites of the

adsorbent, as both compounds: BPA and CV can form inclusion complexes with CD cavity (García-Río et al., 2005; Yang et al., 2008). Although, 1:1 complexes of BPA with β-CD have higher association constant than respective complexes with CV ($3.5 \times 10^4$ $M^{-1}$ vs. $4.7 \times 10^3$ $M^{-1}$) larger CV molecules may be a steric hindrance for host-guest interactions between BPA and CD (Kitano et al., 2003; Nguyen et al., 2013), thus in the binary system BPA sorption was slightly less effective. The increased sorption efficiency of CV observed in the tandem experiments may result from additional sorption sites provided by previously adsorbed pollutant. The extension of the phase contact time from 10 to 20 min had insignificant influence on adsorption efficiency, but under conditions, in which 30 mg of the adsorbent were used the pollutants removal was on the same level as the best results obtained in the single-component solution.

### 3.2.2. Effect of the contact time and adsorption kinetics

To determine the suitable time of contact between the sorption material and pollutants a set of experiments were carried out (Fig. 3b). It was observed that in both cases less than 1 min was required to reach the equilibrium. The maximum amount of BPA and CV adsorbed under the experimental conditions were 32.6 and 16.5 mg $g^{-1}$ respectively. In order to examine the controlling mechanism of adsorption process the pseudo-first, pseudo-second and Avrami fractional-order kinetic models were used to study the experimental data. In kinetic tests 30 mg of BAN-EPI-CDP per sample were used. The parameters obtained for the models are presented in Table S6. In the case of the tests carried out for BPA better fit was observed for pseudo-second (Fig. S9a,b) than for pseudo-first and Avrami fractional-order models, what may suggest that a mechanism of inclusion complex formation between CD cavity and a phenyl ring of BPA is a rate controlling process in this system. The estimated rate constant of BPA adsorption, $k_2$, is 1.42 g $mg^{-1}$ $min^{-1}$. This value is similar to findings described by Alsbaiee et al. (2016) for β-CD polymers cross-linked with tetrafluoroterephthalonitrile, and much higher than these for activated carbons (Brita filters, DARCO, Norit RO 0.8) tested in that work. In the case of CV adsorption a good fit was obtained for both pseudo-first and pseudo-second order models, however a higher regression coefficient in a wider time range was determined for the last mentioned. Moreover, the calculated qe value obtained from pseudo-first order model is much lower than the experimental value indicating that the sorption process is not likely to obey the proposed model, even if the plot has a high correlation coefficient with experimental data (Crini et al., 2007). For this reason, the pseudo-second order model was here also chosen as more appropriate. Similar findings for CV adsorption by β-CD polymer were described by (Chen et al. (2019b), however the reported here process was much faster ($k_2$: 0.50 vs. $6.41 \times 10^{-4}$ $min^{-1}$). The calculated $k_2$ value for CV sorption by BAN-EPI-CDP is almost three times lower comparing with results obtained for BPA, what points out that the non-ionic pollutant is adsorbed much faster than the cationic dye. It can be connected with the strength of the inclusion complex formation (K of BPA-CD complex ~7.5 times higher than for CV-CD). Worst fitness of experimental data for both pollutants to the Avrami model indicates that in adsorption process no phase transformation is involved.

Due to the fact that adsorption is a multi-step process involving a solute transport and diffusion into the sorbent pores, the intraparticle diffusion model was also taken into considerations. Results obtained for BPA and CV, shown in Fig. S9c, reveal a linear relationship between the amount of adsorbed pollutant and the square root of time with the correlation coefficients ($R^2$) equal to 0.99 and 0.98, respectively. This good fit of the model to the experimental data may suggest that the transport of the adsorbate to the pores of BAN-EPI-CDP material is the rate-controlling step, however in both cases the determined values of C constant are not equal to zero. This means that the intraparticle diffusion is not the only rate-controlling step (Weber and Morris, 1963) and also other processes, like inclusion complex formation with BPA and CV have significant influence.

### 3.2.3. Adsorption equilibrium

The Langmuir, Freundlich, and Sips isotherm models were used to describe the equilibrium isotherm data. The fitting curves and adsorption parameters are presented in Fig. 4 and Table 1. The comparison of correlation coefficients ($R^2$) values of the linear fitting indicates a worse fit for the Freundlich model ($R^2 = 0.79$ for BPA and $R^2 = 0.93$ for CV) than for the Langmuir model ($R^2 = 0.99$ for BPA and $R^2 = 0.99$ for CV) to the experimental equilibrium adsorption data. These results suggest that in the process of adsorption mainly monolayer on a relatively homogeneous surface is formed (Liu et al., 2011). The Langmuir model assumes that the adsorption takes place at definite and localized sites and all the adsorption sites are energetically identical. The presence of homogeneous adsorption sites in the BAN-EPI-CDP surface was also indicated by SEM analysis (Fig. 2c). For deeper investigation Sips model, being a combination of Langmuir and Freundlich isotherms, was also applied. As shown in Table 1 the model describes better BPA sorption than the Freundlich model, however the fitness is worse when compare to Langmuir isotherm. Finally, based on the obtained results, the Langmuir model was chosen as the most reliable to describe the BPA and CV removal from water by BAN-EPI-CDP.

According to the Langmuir model adsorption, to classify isotherm shape the dimensionless constant separation factor ($R_L$) was calculated using Eq. (10). The obtained $R_L$ values yielding between 0 and 1 indicate that, the adsorption process between the BAN-EPI-CDP and BPA and CV is favorable. In addition, higher $R_L$ values that have been observed at lower initial concentrations of BPA and CV, showed that adsorption is more favorable at lower concentrations (Crini et al., 2007).

The monolayer saturation capacity, $q_{max}$, was found to be 113.6 mg $g^{-1}$ and 43.1 mg $g^{-1}$ for BPA and CV, respectively. These values of the obtained $q_{max}$ were compared with the maximum sorption capacities of other sorbent materials for BPA reported in the literature and the results are summarized in Table 2. Among presented results higher value of $q_{max}$ have only HCP(BnCD-DCX) and β-CD-TFP sorbents, however for these materials longer contact time, i.e. 30 min was required to achieve high sorption efficiency, whereas for described here sorbent less than 1 min was sufficient.

### 3.2.4. Thermodynamic analysis

In order to assess whether BPA and CV sorption is a spontaneous process the thermodynamic parameters were determined using van't Hoff equation (Eq. 12, Fig. S11). As shown in Table 3 both BPA and CV adsorption is an exothermic process ($\Delta H^0 < 0$), during which the increase of disorder on the solid-liquid interface occurs ($\Delta S^0 < 0$). The negative values of standard Gibbs free energy ($\Delta G^0$) indicate that in both cases sorption is spontaneous and favorable.

### 3.2.5. Effect of pH, ionic strength and humic acids concentration

Due to the fact, that pH can have importance in adsorption process, the influence of its change on the model pollutants uptakes was tested (Fig. 5a). On the basis of the obtained results it can be concluded that the variations in the compounds uptakes in the pH range 4–10 are rather small. In more acidic conditions efficiency of both BPA and CV adsorption is slightly lower, what can be a consequence of the compounds protonation. The solution pH can also influence the adsorption process by changing the surface charge of an adsorbent. For instance, Qu et al. (2020b) in their studies of Pb(II), Cd(II) and Ni(II) adsorption on the microwave functionalized cellulose fibers found the adsorbent surface charge changed from electropositive in acidic to electronegative in alkaline conditions. Therefore, it is possible that in our study also nature of BAN-EPI-CDP in strongly acidic conditions causes weakening of interaction between adsorbate and adsorbent. Above pH 10 BPA uptake decreases significantly (c.a. 2 times lower value). It is possible that in strongly alkaline solution deprotonation of BPA hydroxyl groups takes place. Since these groups are involved in inclusion complex formation (Yang et al., 2008) their deprotonation disturbs hydrogen interactions with CD cavity. Conducting studies in strongly alkaline solutions of CV

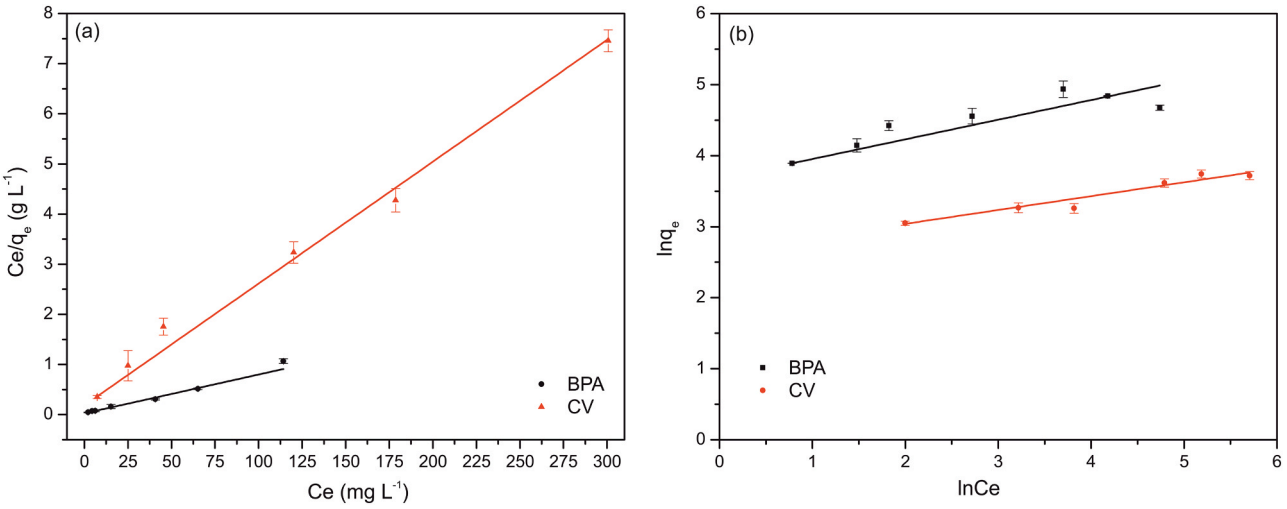


**Fig. 4.** (a) Langmuir and (b) Freundlich isotherm models of BPA (c = 2.2–114.2 mg $L^{-1}$, $m_{sor}$ = 1 mg) and CV (c = 7.4–300.7 mg $L^{-1}$, $m_{sor}$ = 3 mg) adsorption by BAN-EPI-CDP ($t_{contact}$ = 20 min).

**Table 1**
The isotherm parameters for the adsorption of BPA by BAN-EPI-CDP.

| Equilibrium model | Parameter | Value | |
|---|---|---|---|
| | | BPA | CV |
| Langmuir | $q_{max}$ (mg $g^{-1}$) | 113.64 | 43.10 |
| | $K_L$ (L $g^{-1}$) | 111.11 | 2.59 |
| | $a_L$ (L $mg^{-1}$) | 0.98 | 0.06 |
| | $R_L$ | 0.01–0.32 | 0.05–0.69 |
| | $R^2$ | 0.98 | 0.99 |
| Freundlich | $K_F$ ($mg^{1-1/n}$ $L^{1/n}$ $g^{-1}$) | 48.12 | 13.59 |
| | $n_F$ | 4.46 | 4.95 |
| | $R^2$ | 0.75 | 0.92 |
| Sips | $K_s$ [$(mg\ L^{-1})^{-1/ns}$] | 0.53 | 0.18 |
| | $n_s$ | 1.60 | 2.65 |
| | $R^2$ | 0.92 | 0.92 |

**Table 2**
The maximum adsorption capacities ($q_{max}$) reported in the literature for BPA obtained on different cyclodextrin-based adsorbents.

| Polymer | $q_{max}$ (mg $g^{-1}$) | Reference |
|---|---|---|
| HCP(BnCD-DCX) | 278 | (Li et al., 2018) |
| β-CD-TFP | 164.4 | (Zhou et al., 2019) |
| BAN-EPI-CDP | 113.6 | This work |
| β-CD-DFDS | 113.0 | (Wang et al., 2017) |
| β-CA-PDMAEMA | 94.1 | (Zhou et al., 2018) |
| β-CD-TFP | 88.0 | (Alsbaiee et al., 2016) |
| β-CD-MNPs | 74.6 | (Gong et al., 2016) |
| β-CD-CNF | 50.4 | (Lv et al., 2021) |
| β-CD-CMCh | 38.1 | (Kono et al., 2015) |
| β-CD-TFP-CM | 34.7 | (Alzate-Sánchez et al., 2019) |
| β-CD-TFP-CT | 16.5 | (Alzate-Sánchez et al., 2016) |

DCX-dichloroxylene; TFP- tetrafluototerephthalonitrile; DFDS- 4,4′-difluorodiphenylsulfone; CA- citric acid; PDMAEMA- 2-dimethylamino ethyl methacrylate monomer; MNPs- magnetic nanoparticles; CNF- cellulose nanofiber membrane; CMCh- carboxymethylcellulose; CM- cellulose microcrystals; CT-cotton.

**Table 3**
Thermodynamic parameters for BPA and CV adsorption on BAN-EPI-CDP.

| Pollutant | $\Delta G^0$ (kJ $mol^{-1}$) | $\Delta H^0$ (kJ $mol^{-1}$) | $\Delta S^0$ (J $mol^{-1}$ $K^{-1}$) |
|---|---|---|---|
| BPA | -27.09 | -7.10 | 64.90 |
| CV | -11.18 | -9.58 | 45.75 |

was not possible as the excess of hydroxyl ions causes structural changes of CV molecules being a consequence of nucleophilic attack of $OH^-$ on carbon atom connected with aromatic rings (Adams and Rosenstbin, 1914; Begum et al., 1970).

Ionic strength may have a significant influence on adsorption process due to disruption of electrostatic interactions between absorbents and adsorbates. Sodium chloride was used as a model salt to study the effect of ionic strength on BPA and CV adsorption. As shown in Fig. 5b the increase of NaCl concentration did not influence significantly on BPA and CV uptakes. For BPA and CV absorption, only 3.2% and 4.1% of decrement in the removal efficiency was observed, respectively. These results may suggest, that the adsorption of the pollutants is both controlled by hydrogen bonds and hydrophobic effects. In the case, when only hydrogen interactions are the driving force in a complex formation, the increased NaCl concentration causes that the adsorption is less effective due to salting-out of hydrogen bonds. On the other hand, if adsorption is mainly based on hydrophobic effects, the increase of NaCl concentration should enhance BPA and CV sorption as a result of salt-induced dehydration of the hydrated pollutants molecules and a surface of cyclodextrin-bearing materials (Xu et al., 2019). Additionally, the effect of common co-existing ions in real wastewater on the pollutants uptake was studied (Fig. S12). The presence of calcium and copper (II) cations (as chloride salts) as well as carbonate and sulfate(VI) anions (as sodium salts) did not influence significantly on sorption effectiveness. The removal efficiency of BPA and CV slightly decreased in the presence of tested anions, however was still high enough (above 90%) to consider proposed here material for practical applications.

Humic acids (HA) are a naturally occurring mixture of macromolecules, which are ubiquitous in the environment. As HA may compete in the adsorption process (Lim et al., 2015; Zhang et al., 2012), their effect on BPA and CV sorption was tested. On the basis of results shown in Fig. 5c it can be concluded that the presence of HA has a rather insignificant influence on the model pollutants sorption. At HA concentration of 10 mg $L^{-1}$ removal efficiency of BPA slightly decreased from 96.6% to 95.3%, while in the case of CV sorption this value marginally increased from 99.1% to 99.4%. Taking into account that HA are large molecules with a lot of functional groups like hydroxyl, carboxyl, and carbonyl (Schulten and Schnitzer, 1993) one of the possible mechanisms of HA interactions with BAN-EPI-CDP may be the formation of hydrogen bonds, whereas the pore filling can be rather excluded due to too small pore size of the sorption material. As BPA and CV are mainly adsorbed in CD cavities and other hydrophobic sites of the network in CD-bearing materials (Lv et al., 2021; Moradi Shahrebabak et al., 2020; Wang et al., 2020), HA does not compete with the model pollutants for the

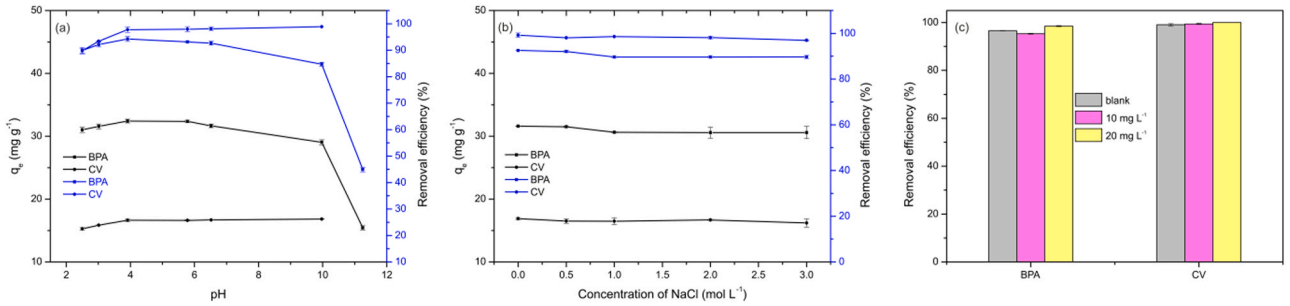


**Fig. 5.** Effect of (a) pH, (b) ionic strength and (c) humic acids concentration on adsorption of BPA (c = 68.5 mg $L^{-1}$, $m_{sor}$ = 10 mg) and CV (c = 102.0 mg $L^{-1}$, $m_{sor}$ = 30 mg) by BAN-EPI-CDP ($t_{contact}$ = 20 min).

binding sites on the surface of the sorption material.

### 3.2.6. *Regeneration experiments*

The effectiveness and economy of the removal of organic pollutants from water effluent make that regeneration of the sorption material is an important issue for practical applications (Qu et al., 2020a). Therefore, the sequential experiments were carried out to test the reusability of BAN-EPI-CDP as shown in Fig. 6. In contrast to energy-consuming and degradative regeneration of activated carbons, BPA could be easily removed from the sorbent by soaking the material in methanol at room temperature. Five consecutive cycles of BPA adsorption/desorption shown no significant decrease in the material removal efficiency. Although, the desorption of CV was more time-consuming than in the case of BPA, the regenerated material could be used at least five times without significant loss in the dye removal efficiency. Moreover, methanol could be easily separated from the pollutants after desorption process and reused in next cycle, what influences on economy of the protocol. The pollutants after the sorbent regeneration can be further treated. An interesting example of BPA removal is its photodegradation with the utilization of β-CD-modified photocatalysts described by Zhou et al. (2020). Although proposed in that work photocatalysts ensured high efficiency of BPA degradation, one should keep in mind the toxicity of intermediates obtained in an oxidation system, as some of BPA photodegradation products can pose a greater environmental risk than the target pollutant (Chiang et al., 2004).

### 3.2.7. *Environmental applications*

As natural water reservoirs and wastewaters are a complex mixture of various compounds, sorption materials considered for practical applications should remove pollutants effectively despite interfering background (Zhang et al., 2021). To assess the potential in the treatment of waters containing BPA and CV pollutants, adsorption was performed under real conditions (water from a pond in the Oruński Park) using BAN-EPI-CDP as an adsorbent. As presented in Fig. 7a, related to the adsorption results of model pollutants effluents, in the real conditions the BAN-EPI-CDP exhibited comparable adsorption efficiency values. The results of simulated and real effluents showed that BAN-EPI-CDP material has significant potential in the treatment of effluents containing BPA and CV toxic pollutants.

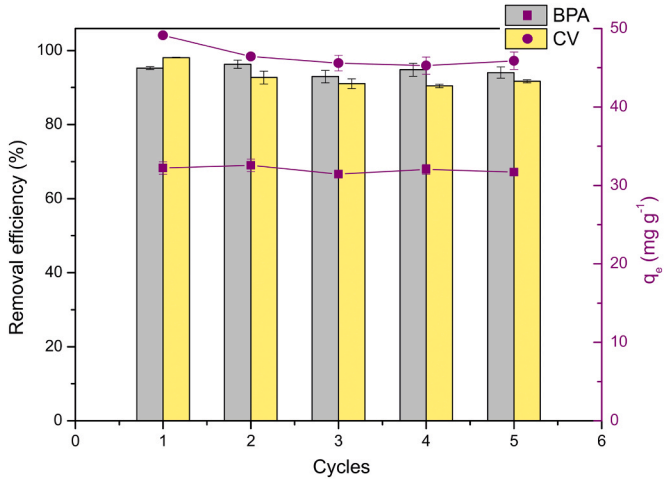


**Fig. 6.** The average efficiency of BPA (c = 68.5 mg $L^{-1}$, $m_{sor}$ = 10 mg) and CV (c = 102.0 mg $L^{-1}$, $m_{sor}$ = 30 mg) removal by BAN-EPI-CDP after consecutive regeneration cycles.

### 3.2.8. *Adsorption experiments of ionic and non-ionic pollutants through different type of adsorbents*

The experiments of the adsorption were performed for the uptake of selected ionic and non-ionic pollutants through various types of adsorbents: BAN, EPI-CDP and BAN-EPI-CDP. As presented in Fig. 7b, the BAN-EPI-CDP showed the best adsorption efficiency results for cationic dyes and non-ionic compounds. Comparing to BAN-EPI-CDP, the EPI-CDP had better adsorption efficiency results for anionic dye (CR) and comparable results of some non-ionic compounds: BPA and 4-HB. Finally, even though BAN had relatively high adsorption efficiency values for cationic dyes, these values for anionic dye and non-ionic pollutants were significantly lower compared to EPI-CDP and BAN-EPI-CDP. According to the results, it can be concluded that it was reasonable to combine the functions of the adsorption properties of BAN and EPI-CDP materials, because it allowed to obtain high values of the adsorption efficiency for a much wider range of pollutants than the raw materials.

### 3.2.9. *Removal of pollutants from a complex mixture by the BAN-EPI-CDP*

To evaluate the possibility of simultaneous removal of different pollutants, the adsorption by BAN-EPI-CDP was performed on a model mixture of pollutants. Ionic: CV, MB, NR, CA and non-ionic: 2-NP, BPA and 4-H compounds, were selected in terms of the maximum wavelength ($\lambda_{max}$) values, so that they could be easily identified using the UV-Vis spectrophotometry, before and after the adsorption process (Fig. 7c inserted). As shown in Fig. 7c, the adsorption efficiency (AE) of selected pollutants in complex mixtures was relatively on the same level for CV, CA, NR, BPA (the change of AE comparing single and multi-components solutions $\Delta AE \leq 11\%$), slightly lower for MB and 4-HB ($11\% < \Delta AE < 20\%$) or much lower for 2-NP ($\Delta AE > 20\%$) than AE values obtained from single pollution adsorption. The lower values of adsorption efficiency were caused by the competitive mechanism of sorption of simultaneously occurring pollutants in a complex mixture. The significantly lower values of AE observed for 2-NP could be additionally caused by the relatively small molecular size of the compound that could not be adsorbed in the mesopores, which constitute the main part of the surface area of the BAN-EPI-CDP material (Fig. S7). The BAN-EPI-CDP material retained selectivity in the complex mixture of pollutants with respect to cationic and non-ionic compounds exactly as in a single pollution adsorption process resulting in high efficiency of adsorption

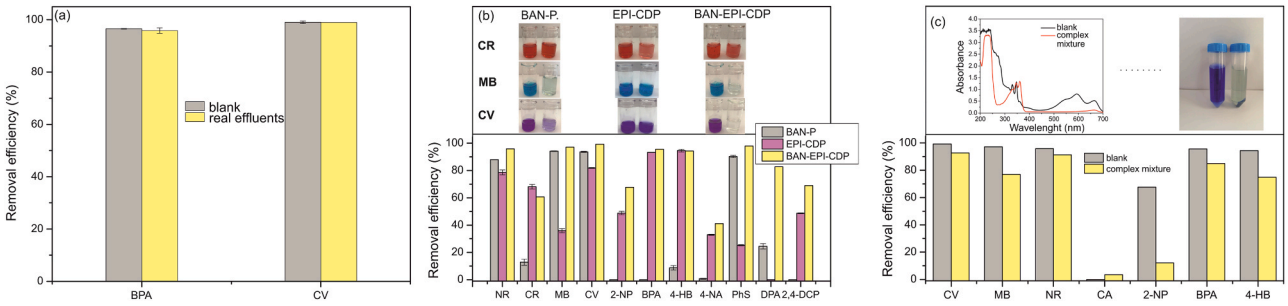


**Fig. 7.** Removal efficiency of selected pollutants (a) in real effluents by BAN-EPI-CDP (BPA: c = 68.5 mg $L^{-1}$, $m_{sor}$ = 10 mg; CV: c = 102.0 mg $L^{-1}$, $m_{sor}$ = 30 mg), (b) through different type of adsorbents ($c_{pollutant\ ionic}$ = 0.05 mM, $c_{pollutant\ non\text{-}ionic}$ = 0.5 mM, $m_{sor}$ = 30 mg) and (c) in complex mixtures ($c_{pollutant}$ = 0.3 mM, $m_{sor}$ = 250 mg) by BAN-EPI-CDP ($t_{contact}$ = 20 min).

values. Based on the obtained results, we can conclude that BAN-EPI-CDP material has great ability to selective and simultaneous removal of different pollutants and can be potentially incorporated on a larger scale.

### 3.2.10. *Proposed mechanism of BPA and CV removal*

Taking into account all above considerations it can be postulated that the BPA and CV sorption on BAN-EPI-CDP is a complex process involving the formation of inclusion complexes between target pollutants and CD cavity, hydrogen interactions and physical sorption in the sorbent network. Analysis of sorption kinetics and FTIR spectra of the sorbent registered in the presence of BPA or CV (Fig. S13) suggests that host-guest interactions play a major role in the pollutants uptake. A shift of bands corresponding to hydroxyl –OH stretching vibrations and H-O-H deformation bending of water molecules, that can be found in the spectrum of the sorption material at 3423 and 1637 $cm^{-1}$, to higher wavenumbers in the presence of the pollutants suggests disappearance of water molecule from CD cavity (Chen et al., 2019b). Similar phenomenon is observed in the case of inclusion complexes with native cyclodextrins (Egyed and Weiszfeiler, 1994). Additionally, in the spectrum with adsorbed BPA, changes seen in the region of C-O-C and C-OH stretching vibrations suggest involvement of hydrogen interactions between OH groups of CD and BPA molecule. Changes of intensity of the C-H deformation vibration bands in the primary and secondary hydroxyl groups of CD can be a consequence of inclusion of BPA aromatic ring into CD cavity stabilized by hydrogen bridges. The higher adsorption capacity of the sorption material for BPA than for CV determined from adsorption isotherm studies may be a results of higher affinity of β-CD, included in the material, to the non-ionic pollutants.

## 4. Conclusions

In this study, we designed and synthesized a novel, environmental-friendly biomass-derived β-CD-based material (BAN-EPI-CDP) by copolymerization of β-CD with epichlorohydrin and cellulose obtained from banana peels. The characterization analysis (FTIR, XRD, EA, SEM) showed that the material of an amorphous structure contains around 53% of β-CD and its surface is dominated by mesopores with pore size range of 2–50 nm. Ionic CV and non-ionic BPA were selected as model pollutants to study the adsorption performance of BAN-EPI-CDP. The results showed that the sorption material can rapidly and simultaneously remove these pollutants with high efficiency in pH range 4–10 without being affected by ionic strength and humic acid concentration, what indicates that BAN-EPI-CDP can be a suitable material for real-water treatment. The kinetic and isotherms studies pointed out that the adsorption of BPA and CV takes place on a relatively homogeneous surface. The estimated rate constant of pseudo-second order process for BPA sorption was almost three times higher comparing with results obtained for CV, what means that the non-ionic pollutant is adsorbed much faster than the cationic dye. The adsorption equilibrium data of the material for BPA and CV were fitted well by the Langmuir equation showing a maximum absorption capacity of 113.6 mg $g^{-1}$ and 43.1 mg $g^{-1}$, respectively. After pollutant sorption, BAN-EPI-CDP could be easily regenerated under mild conditions and used at least five times without significant loss of removal efficiency. The easy and green preparation, high sorption efficiency towards hazardous organic pollutants and good regeneration performance make BAN-EPI-CDP a promising alternative to commercially used activated carbons for water treatment.

## CRediT authorship contribution statement

**Koleta Hemine**: Conceptualization, Methodology, Investigation, Formal analysis, Validation, Writing - original draft, Visualization, Writing - review & editing. **Natalia Łukasik**: Conceptualization, Methodology, Investigation, Formal analysis, Validation, Writing - original draft, Visualization, Writing - review & editing. **Maria Gazda**: Investigation, Formal analysis, Writing - review & editing. **Izabela Nowak**: Investigation, Formal analysis, Writing - review & editing.

## Declaration of Competing Interest

The authors declare that they have no known competing financial interests or personal relationships that could have appeared to influence the work reported in this paper.

## Acknowledgements

The authors are grateful for financial support provided by Gdańsk University of Technology, DS 034718. This research was supported by grant from Gdańsk University of Technology, Poland (grant number: 033880). The authors would like to thank MSc Dominika Sołtyszewska and Ph.D. Mariusz Szkoda for help in the experimental work.

## Appendix A. Supporting information

Supplementary data associated with this article can be found in the online version at doi:10.1016/j.jhazmat.2021.126286.

## References

Adams, E.Q., Rosenstbin, L., 1914. The color and ionization of crystal-violet. J. Am. Chem. Soc. 36, 1452–1473. https://doi.org/10.1021/ja02184a014.

Afkhami, A., Saber-Tehrani, M., Bagheri, H., 2010. Modified maghemite nanoparticles as an efficient adsorbent for removing some cationic dyes from aqueous solution. Desalination 263, 240–248. https://doi.org/10.1016/j.desal.2010.06.065.

Afolabi, F.O., Musonge, P., Bakare, B.F., 2021. Bio-sorption of copper and lead ions in single and binary systems onto banana peels. Cogent Eng. 8, 1886730 https://doi.org/10.1080/23311916.2021.1886730.

Akpomie, K.G., Conradie, J., 2020. Banana peel as a biosorbent for the decontamination of water pollutants. A review. Environ. Chem. Lett. 18, 1085–1112. https://doi.org/10.1007/s10311-020-00995-x.

Ali, A., 2017. Removal of Mn(II) from water using chemically modified banana peels as efficient adsorbent. Environ. Nanotechnol. Monit. Manag. 7, 57–63. https://doi.org/10.1016/j.enmm.2016.12.004.
Ali, I., Gupta, V.K., 2007. Advances in water treatment by adsorption technology. Nat. Protoc. 1, 2661–2667. https://doi.org/10.1038/nprot.2006.370.
Alsbaiee, A., Smith, B.J., Xiao, L., Ling, Y., Helbling, D.E., Dichtel, W.R., 2016. Rapid removal of organic micropollutants from water by a porous β-cyclodextrin polymer. Nature 529, 190–194. https://doi.org/10.1038/nature16185.
Alzate-Sánchez, D.M., Ling, Y., Li, C., Frank, B.P., Bleher, R., Fairbrother, D.H., Helbling, D.E., Dichtel, W.R., 2019. β-cyclodextrin polymers on microcrystalline cellulose as a granular media for organic micropollutant removal from water. ACS Appl. Mater. Interfaces 11, 8089–8096. https://doi.org/10.1021/acsami.8b22100.
Alzate-Sánchez, D.M., Smith, B.J., Alsbaiee, A., Hinestroza, J.P., Dichtel, W.R., 2016. Cotton fabric functionalized with a β-cyclodextrin polymer captures organic pollutants from contaminated air and water. Chem. Mater. 28, 8340–8346. https://doi.org/10.1021/acs.chemmater.6b03624.
Barrett, E.P., Joyner, L.G., Halenda, P.P., 1951. The determination of pore volume and area distributions in porous substances. I. Computations from nitrogen isotherms. J. Am. Chem. Soc. 73, 373–380. https://doi.org/10.1021/ja01145a126.
Begum, F., Molla, M.Y.A., Rahman, M.M., Susan, M.A.B.H., 1970. Kinetics of the alkaline hydrolysis of crystal violet in micelles, reverse micelles and microemulsions of cetyltrimethylammonium bromide. J. Bangladesh Chem. Soc. 24, 173–184. https://doi.org/10.3329/jbcs.v24i2.9706.
Bernhardt, E.S., Rosi, E.J., Gessner, M.O., 2017. Synthetic chemicals as agents of global change. Front. Ecol. Environ. 15, 84–90. https://doi.org/10.1002/fee.1450.
Bhatnagar, A., Minocha, A.K., 2006. Conventional and non-conventional adsorbents for removal of pollutants from water - a review. Indian J. Chem. Technol. 13, 203–217.
Brunauer, S., Emmett, P.H., Teller, E., 1938. Adsorption of gases in multimolecular layers. J. Am. Chem. Soc. 60, 309–319. https://doi.org/10.1021/ja01269a023.
Chen, B., Chen, S., Zhao, H., Liu, Y., Long, F., Pan, X., 2019a. A versatile B-cyclodextrin and polyethyleneimine bi-functionalized magnetic nanoadsorbent for simultaneous capture of methyl orange and Pb(II) from complex wastewater. Chemosphere 216, 605–616. https://doi.org/10.1016/j.chemosphere.2018.10.157.
Chen, J., Liu, M., Pu, Y., Wang, C., Han, J., Jiang, M., Liu, K., 2019b. The preparation of thin-walled multi-cavities β-cyclodextrin polymer and its static and dynamic properties for dyes removal. J. Environ. Manag. 245, 105–113. https://doi.org/10.1016/j.jenvman.2019.04.125.
Cheng, M., Ma, W., Li, J., Huang, Y., Zhao, J., Wen, Y.X., Xu, Y., 2004. Visible-light-assisted degradation of dye pollutants over Fe(III)-loaded resin in the presence of $H_2O_2$ at neutral pH values. Environ. Sci. Technol. 38, 1569–1575. https://doi.org/10.1021/es034442x.
Chiang, K., Lim, T.M., Tsen, L., Lee, C.C., 2004. Photocatalytic degradation and mineralization of bisphenol A by $TiO_2$ and platinized $TiO_2$. Appl. Catal. A Gen. 261, 225–237. https://doi.org/10.1016/j.apcata.2003.11.004.
Crini, G., 2014. Review: a history of cyclodextrins. Chem. Rev. 114, 10940–10975. https://doi.org/10.1021/cr500081p.
Crini, G., Peindy, H.N., Gimbert, F., Robert, C., 2007. Removal of C.I. Basic Green 4 (Malachite Green) from aqueous solutions by adsorption using cyclodextrin-based adsorbent: kinetic and equilibrium studies. Sep. Purif. Technol. 53, 97–110. https://doi.org/10.1016/j.seppur.2006.06.018.
Egyed, O., Weiszfeiler, V., 1994. Structure determination of copper(II)-β-cyclodextrin complex by Fourier transform infrared spectroscopy. Vib. Spectrosc. 7, 73–77. https://doi.org/10.1016/0924-2031(94)85042-9.
Gao, X., Kang, S., Xiong, R., Chen, M., 2020. Environment-friendly removal methods for endocrine disrupting chemicals. Sustainability 12, 1–16. https://doi.org/10.3390/su12187615.
García-Río, L., Godoy, A., Leis, J.R., 2005. Spectroscopic characterisation of crystal violet inclusion complexes in β-cyclodextrin. Chem. Phys. Lett. 401, 302–306. https://doi.org/10.1016/j.cplett.2004.11.063.
Gong, T., Zhou, Y., Sun, L., Liang, W., Yang, J., Shuang, S., Dong, C., 2016. Effective adsorption of phenolic pollutants from water using β-cyclodextrin polymer functionalized $Fe_3O_4$ magnetic nanoparticles. RSC Adv. 6, 80955–80963. https://doi.org/10.1039/c6ra16383a.
Guo, R., Wang, R., Yin, J., Jiao, T., Huang, H., Zhao, X., Zhang, L., Li, Q., Zhou, J., Peng, Q., 2019. Fabrication and highly efficient dye removal characterization of beta-cyclodextrin-based composite polymer fibers by electrospinning. Nanomaterials 9, 127. https://doi.org/10.3390/nano9010127.
Hall, K.R., Eagleton, L.C., Acrivos, A., Vermeulen, T., 1966. Pore- and solid-diffusion kinetics in fixed-bed adsorption under constant-pattern conditions. Ind. Eng. Chem. Fundam. 5, 212–223. https://doi.org/10.1021/i160018a011.
Hassaan, M.A., El Nemr, A., Madkour, F.F., 2017. Testing the advanced oxidation processes on the degradation of Direct Blue 86 dye in wastewater. Egypt. J. Aquat. Res. 43, 11–19. https://doi.org/10.1016/j.ejar.2016.09.006.
Ho, Y.S., McKay, G., 1998. Kinetic models for the sorption of dye from aqueous solution by wood. Trans. IChemE 76, 183–191. https://doi.org/10.1205/095758298529326.
Ho, Y.S., Porter, J.F., Mckay, G., 2002. Equilibrium isotherm studies for the sorption of divalent metal ions onto peat: copper, nickel, and lead single component systems. Water Air Soil Pollut. 141, 1–33.
Hu, J.Y., Aizawa, T., Ookubo, S., 2002. Products of aqueous chlorination of bisphenol A and their estrogenic activity. Environ. Sci. Technol. 36, 1980–1987. https://doi.org/10.1021/es011177b.
Hu, X., Hu, Y., Xu, G., Li, M., Zhu, Y., Jiang, L., Tu, Y., Zhu, X., Xie, X., Li, A., 2020. Green synthesis of a magnetic β-cyclodextrin polymer for rapid removal of organic micro-pollutants and heavy metals from dyeing wastewater. Environ. Res. 180, 108796 https://doi.org/10.1016/j.envres.2019.108796.
Huang, J.H., Huang, K.L., Liu, S.Q., Wang, A.T., Yan, C., 2008. Adsorption of Rhodamine B and methyl orange on a hypercrosslinked polymeric adsorbent in aqueous solution. Colloids Surf. A Physicochem. Eng. Asp. 330, 55–61. https://doi.org/10.1016/j.colsurfa.2008.07.050.
Huang, W., Hu, Y., Li, Y., Zhou, Y., Niu, D., Lei, Z., Zhang, Z., 2018. Citric acid-crosslinked β-cyclodextrin for simultaneous removal of bisphenol A, methylene blue and copper: the roles of cavity and surface functional groups. J. Taiwan Inst. Chem. Eng. 82, 189–197. https://doi.org/10.1016/j.jtice.2017.11.021.
Işik, M., Sponza, D.T., 2008. Anaerobic/aerobic treatment of a simulated textile wastewater. Sep. Purif. Technol. 60, 64–72. https://doi.org/10.1016/j.seppur.2007.07.043.
Jamee, R., Siddique, R., 2019. Biodegradation of synthetic dyes of textile effluent by microorganisms: an environmentally and economically sustainable approach. Eur. J. Microbiol. Immunol. 9, 114–118. https://doi.org/10.1556/1886.2019.00018.
Jia, Z., Li, Z., Li, S., Li, Y., Zhu, R., 2016. Adsorption performance and mechanism of methylene blue on chemically activated carbon spheres derived from hydrothermally-prepared poly(vinyl alcohol) microspheres. J. Mol. Liq. 220, 56–62. https://doi.org/10.1016/j.molliq.2016.04.063.
Khalafi, L., Kashani, S., Karimi, J., 2016. Molecular recognition: detection of colorless compounds based on color change. J. Chem. Educ. 93, 376–379. https://doi.org/10.1021/acs.jchemed.5b00232.
Kitano, H., Endo, H., Gemmei-Ide, M., Kyogoku, M., 2003. Inclusion of bisphenols by cyclodextrin derivatives. J. Incl. Phenom. Macrocycl. Chem. 47, 83–90. https://doi.org/10.1023/B:JIPH.0000003879.99301.cd.
Kono, H., Nakamura, T., Hashimoto, H., Shimizu, Y., 2015. Characterization, molecular dynamics, and encapsulation ability of β-cyclodextrin polymers crosslinked by polyethylene glycol. Carbohydr. Polym. 128, 11–23. https://doi.org/10.1016/j.carbpol.2015.04.009.
Kortenkamp, A., Faust, M., 2018. Regulate to reduce chemical mixture risk. Science 361, 224–226. https://doi.org/10.1126/science.aat9219.
Kos, L., Perkowski, J., 2003. Decolouration of real textile wastewater with advanced oxidation processes. Fibres Text. East. Eur. 11, 81–85.
Kozlowski, C.A., Sliwa, W., 2008. The use of membranes with cyclodextrin units in separation processes: recent advances. Carbohydr. Polym. 74, 1–9. https://doi.org/10.1016/j.carbpol.2008.01.010.
Lagergren, S., 1898. About the theory of so-called adsorption of soluble substances. K. Sven. Vetensk. Handl. 24, 1–39.
Li, M., Wang, X., Porter, C.J., Cheng, W., Zhang, X., Wang, L., Elimelech, M., 2019. Concentration and recovery of dyes from textile wastewater using a self-standing, support-free forward osmosis membrane. Environ. Sci. Technol. 53, 3078–3086. https://doi.org/10.1021/acs.est.9b00446.
Li, X., Zhou, M., Jia, J., Ma, J., Jia, Q., 2018. Design of a hyper-crosslinked B-cyclodextrin porous polymer for highly efficient removal toward bisphenol a from water. Sep. Purif. Technol. 195, 130–137. https://doi.org/10.1016/j.seppur.2017.12.007.
Lim, B.R., Do, S.H., Hong, S.H., 2015. The impact of humic acid on the removal of bisphenol A by adsorption and ozonation. Desalin. Water Treat. 54, 1226–1232. https://doi.org/10.1080/19443994.2014.896751.
Lima, É.C., Adebayo, M.A., Machado, F.M., 2015. Kinetic and equilibrium models of adsorption. Carbon Nanostruct. 33–69. https://doi.org/10.1007/978-3-319-18875-1_3.
Lima, E.C., Hosseini-Bandegharaei, A., Moreno-Piraján, J.C., Anastopoulos, I., 2019. A critical review of the estimation of the thermodynamic parameters on adsorption equilibria. Wrong use of equilibrium constant in the Van't Hoof equation for calculation of thermodynamic parameters of adsorption. J. Mol. Liq. 273, 425–434. https://doi.org/10.1016/j.molliq.2018.10.048.
Liu, H., Cai, X., Wang, Y., Chen, J., 2011. Adsorption mechanism-based screening of cyclodextrin polymers for adsorption and separation of pesticides from water. Water Res. 45, 3499–3511. https://doi.org/10.1016/j.watres.2011.04.004.
Liu, Q., Zhou, Yi, Lu, J., Zhou, Yanbo, 2020. Novel cyclodextrin-based adsorbents for removing pollutants from wastewater: a critical review. Chemosphere 241, 125043. https://doi.org/10.1016/j.chemosphere.2019.125043.
Lv, Y., Ma, J., Liu, K., Jiang, Y., Yang, G., Liu, Y., Lin, C., Ye, X., Shi, Y., Liu, M., Chen, L., 2021. Rapid elimination of trace bisphenol pollutants with porous β-cyclodextrin modified cellulose nanofibrous membrane in water: adsorption behavior and mechanism. J. Hazard. Mater. 403, 123666 https://doi.org/10.1016/j.jhazmat.2020.123666.
Mallard, I., Städe, L.W., Ruellan, S., Jacobsen, P.A.L., Larsen, K.L., Fourmentin, S., 2015. Synthesis, characterization and sorption capacities toward organic pollutants of new β-cyclodextrin modified zeolite derivatives. Colloids Surf. A Physicochem. Eng. Asp. 482, 50–57. https://doi.org/10.1016/j.colsurfa.2015.04.014.
McKay, G., 2007. Adsorption of dyestuffs from aqueous solutions with activated carbon I: equilibrium and batch contact-time studies. J. Chem. Technol. Biotechnol. 32, 759–772. https://doi.org/10.1002/jctb.5030320712.
Moradi Shahrebabak, S., Saber-Tehrani, M., Faraji, M., Shabanian, M., Aberoomand-Azar, P., 2020. Magnetic solid phase extraction based on poly(β-cyclodextrin-ester) functionalized silica-coated magnetic nanoparticles (NPs) for simultaneous extraction of the malachite green and crystal violet from aqueous samples. Environ. Monit. Assess. 192, 262. https://doi.org/10.1007/s10661-020-8185-6.
Nabi Bidhendi, G.R., Torabian, A., Ehsani, H., Razmkhah, N., 2007. Evaluation of industrial dyeing wastewater treatment with coagulants and polyelectrolyte as a coagulant aid. Iran. J. Environ. Health Sci. Eng. 4, 29–36.
Nguyen, H.T., Pham, D.T., Easton, C.J., Lincoln, S.F., 2013. Complexation of crystal violet, pyronine B, and rhodamine B by linked β-cyclodextrin trimers. Aust. J. Chem. 66, 1057–1064. https://doi.org/10.1071/CH13172.

Pelissari, F.M., Sobral, P.J.D.A., Menegalli, F.C., 2014. Isolation and characterization of cellulose nanofibers from banana peels. Cellulose 21, 417–432. https://doi.org/10.1007/s10570-013-0138-6.

Petrie, B., Barden, R., Kasprzyk-Hordern, B., 2015. A review on emerging contaminants in wastewaters and the environment: current knowledge, understudied areas and recommendations for future monitoring. Water Res. 72, 3–27. https://doi.org/10.1016/j.watres.2014.08.053.

Pothitou, P., Voutsa, D., 2008. Endocrine disrupting compounds in municipal and industrial wastewater treatment plants in Northern Greece. Chemosphere 73, 1716–1723. https://doi.org/10.1016/j.chemosphere.2008.09.037.

Qin, X., Bai, L., Tan, Y., Li, L., Song, F., Wang, Y., 2019. B-Cyclodextrin-crosslinked polymeric adsorbent for simultaneous removal and stepwise recovery of organic dyes and heavy metal ions: fabrication, performance and mechanisms. Chem. Eng. J. 372, 1007–1018. https://doi.org/10.1016/j.cej.2019.05.006.

Qu, J., Akindolie, M.S., Feng, Y., Jiang, Z., Zhang, G., Jiang, Q., Deng, F., Cao, B., Zhang, Y., 2020a. One-pot hydrothermal synthesis of $NaLa(CO_3)_2$ decorated magnetic biochar for efficient phosphate removal from water: kinetics, isotherms, thermodynamics, mechanisms and reusability exploration. Chem. Eng. J. 394, 124915 https://doi.org/10.1016/j.cej.2020.124915.

Qu, J., Liu, Y., Cheng, L., Jiang, Z., Zhang, G., Deng, F., Wang, L., Han, W., Zhang, Y., 2021a. Green synthesis of hydrophilic activated carbon supported sulfide nZVI for enhanced Pb(II) scavenging from water: characterization, kinetics, isotherms and mechanisms. J. Hazard. Mater. 403, 123607 https://doi.org/10.1016/j.jhazmat.2020.123607.

Qu, J., Meng, Q., Lin, X., Han, W., Jiang, Q., Wang, L., Hu, Q., Zhang, L., Zhang, Y., 2021b. Microwave-assisted synthesis of β-cyclodextrin functionalized celluloses for enhanced removal of Pb(II) from water: adsorptive performance and mechanism exploration. Sci. Total Environ. 752, 141854 https://doi.org/10.1016/j.scitotenv.2020.141854.

Qu, J., Tian, X., Jiang, Z., Cao, B., Akindolie, M.S., Hu, Q., Feng, C., Feng, Y., Meng, X., Zhang, Y., 2020b. Multi-component adsorption of Pb(II), Cd(II) and Ni(II) onto microwave-functionalized cellulose: kinetics, isotherms, thermodynamics, mechanisms and application for electroplating wastewater purification. J. Hazard. Mater. 387, 121718 https://doi.org/10.1016/j.jhazmat.2019.121718.

Rosales, E., Pazos, M., Sanromán, M.A., Tavares, T., 2012. Application of zeolite-Arthrobacter viscosus system for the removal of heavy metal and dye: chromium and Azure B. Desalination 284, 150–156. https://doi.org/10.1016/j.desal.2011.08.049.

Sabio, E., González, E., González, J.F., González-García, C.M., Ramiro, A., Gañan, J., 2004. Thermal regeneration of activated carbon saturated with p-nitrophenol. Carbon 42, 2285–2293. https://doi.org/10.1016/j.carbon.2004.05.007.

Sansuk, S., Srijaranai, Somkiat, Srijaranai, Supalax, 2016. A new approach for removing anionic organic dyes from wastewater based on electrostatically driven assembly. Environ. Sci. Technol. 50, 6477–6484. https://doi.org/10.1021/acs.est.6b00919.

Schulten, H.-R., Schnitzer, M., 1993. A state of the art structural concept for humic substances. Naturwissenschaften 80, 29–30.

Schwarzenbach, R.P., Escher, B.I., Fenner, K., Hofstetter, T.B., Johnson, C.A., Gunten, U., Von, Wehrli, B., 2006. The challenge of micropollutants in aquatic systems. Science 313, 1072–1077.

Shen, H.M., Zhu, G.Y., Yu, W., Bin, Wu, H.K., Ji, H.B., Shi, H.X., She, Y., Bin, Zheng, Y.F., 2015. Fast adsorption of p-nitrophenol from aqueous solution using β-cyclodextrin grafted silica gel. Appl. Surf. Sci. 356, 1155–1167. https://doi.org/10.1016/j.apsusc.2015.08.203.

Spagni, A., Casu, S., Grilli, S., 2012. Decolourisation of textile wastewater in a submerged anaerobic membrane bioreactor. Bioresour. Technol. 117, 180–185. https://doi.org/10.1016/j.biortech.2012.04.074.

Stavrinou, A., Aggelopoulos, C.A., Tsakiroglou, C.D., 2020. A methodology to estimate the sorption parameters from batch and column tests: the case study of methylene blue sorption onto banana peels. Processes 8, 1–22. https://doi.org/10.3390/pr8111467.

Szejtli, J., 1988. Cyclodextrin Technology. Kluwer Academic Publishers, Dordrecht.

Szente, L., Szejtli, J., 2004. Cyclodextrins as food ingredients. Trends Food Sci. Technol. 15, 137–142. https://doi.org/10.1016/j.tifs.2003.09.019.

Thamaraiselvan, C., Noel, M., 2015. Membrane processes for dye wastewater treatment: recent progress in fouling control. Crit. Rev. Environ. Sci. Technol. 45, 1007–1040. https://doi.org/10.1080/10643389.2014.900242.

Vakili, M., Rafatullah, M., Salamatinia, B., Abdullah, A.Z., Ibrahim, M.H., Tan, K.B., Gholami, Z., Amouzgar, P., 2014. Application of chitosan and its derivatives as adsorbents for dye removal from water and wastewater: a review. Carbohydr. Polym. 113, 115–130. https://doi.org/10.1016/j.carbpol.2014.07.007.

Verma, A.K., Dash, R.R., Bhunia, P., 2012. A review on chemical coagulation/flocculation technologies for removal of colour from textile wastewaters. J. Environ. Manag. 93, 154–168. https://doi.org/10.1016/j.jenvman.2011.09.012.

Wang, J., Cheng, G., Lu, J., Chen, H., Zhou, Y., 2020. PDA-cross-linked beta-cyclodextrin: a novel adsorbent for the removal of BPA and cationic dyes. Water Sci. Technol. 81, 2337–2350. https://doi.org/10.2166/wst.2020.286.

Wang, Z., Zhang, P., Hu, F., Zhao, Y., Zhu, L., 2017. A crosslinked β-cyclodextrin polymer used for rapid removal of a broad-spectrum of organic micropollutants from water. Carbohydr. Polym. 177, 224–231. https://doi.org/10.1016/j.carbpol.2017.08.059.

Weber, W.J., Morris, J.C., 1963. Kinetics of adsorption on carbon from solution. J. Sanit. Eng. Div. 89, 31–60.

Xu, G., Xie, X., Qin, L., Hu, X., Zhang, D., Xu, J., Li, D., Ji, X., Huang, Y., Tu, Y., Jiang, L., Wei, D., 2019. Simple synthesis of a swellable porous β-cyclodextrin-based polymer in the aqueous phase for the rapid removal of organic micro-pollutants from water. Green Chem. 21, 6062–6072. https://doi.org/10.1039/c9gc02422k.

Xue, J., Liu, W., Kannan, K., 2017. Bisphenols, benzophenones, and bisphenol A diglycidyl ethers in textiles and infant clothing. Environ. Sci. Technol. 51, 5279–5286. https://doi.org/10.1021/acs.est.7b00701.

Yadav, M., Das, M., Savani, C., Thakore, S., Jadeja, R., 2019. Maleic anhydride cross-linked β-cyclodextrin-conjugated magnetic nanoadsorbent: an ecofriendly approach for simultaneous adsorption of hydrophilic and hydrophobic dyes. ACS Omega 4, 11993–12003. https://doi.org/10.1021/acsomega.9b00881.

Yang, Z.X., Chen, Y., Liu, Y., 2008. Inclusion complexes of bisphenol A with cyclomaltoheptaose (β-cyclodextrin): solubilization and structure. Carbohydr. Res. 343, 2439–2442. https://doi.org/10.1016/j.carres.2008.06.018.

Yuan, Z., Liu, H., Wu, H., Wang, Yiming, Liu, Q., Wang, Yu, Lincoln, S.F., Guo, X., Wang, J., 2020a. Cyclodextrin hydrogels: rapid removal of aromatic micropollutants and adsorption mechanisms. J. Chem. Eng. Data 65, 678–689. https://doi.org/10.1021/acs.jced.9b00913.

Yuan, Z., Liu, H., Wu, H., Wang, Yiming, Liu, Q., Wang, Yu, Lincoln, S.F., Guo, X., Wang, J., 2020b. Cyclodextrin hydrogels : rapid removal of aromatic micropollutants and adsorption mechanisms. J. Chem. Eng. Data 65, 678–689. https://doi.org/10.1021/acs.jced.9b00913.

Yurtsever, A., Sahinkaya, E., Aktaş, Ö., Uçar, D., Çinar, Ö., Wang, Z., 2015. Performances of anaerobic and aerobic membrane bioreactors for the treatment of synthetic textile wastewater. Bioresour. Technol. 192, 564–573. https://doi.org/10.1016/j.biortech.2015.06.024.

Zahrim, A.Y., Hilal, N., 2013. Treatment of highly concentrated dye solution by coagulation/flocculation-sand filtration and nanofiltration. Water Resour. Ind. 3, 23–34. https://doi.org/10.1016/j.wri.2013.06.001.

Zhang, X., Kah, M., Jonker, M.T.O., Hofmann, T., 2012. Dispersion state and humic acids concentration-dependent sorption of pyrene to carbon nanotubes. Environ. Sci. Technol. 46, 7166–7173. https://doi.org/10.1021/es300645m.

Zhang, Y., Akindolie, M.S., Tian, X., Wu, B., Hu, Q., Jiang, Z., Wang, L., Tao, Y., Cao, B., Qu, J., 2021. Enhanced phosphate scavenging with effective recovery by magnetic porous biochar supported $La(OH)_3$: kinetics, isotherms, mechanisms and applications for water and real wastewater. Bioresour. Technol. 319, 124232 https://doi.org/10.1016/j.biortech.2020.124232.

Zhao, F., Repo, E., Yin, D., Meng, Y., Jafari, S., Sillanpää, M., 2015. EDTA-cross-linked β-cyclodextrin: an environmentally friendly bifunctional adsorbent for simultaneous adsorption of metals and cationic dyes. Environ. Sci. Technol. 49, 10570–10580. https://doi.org/10.1021/acs.est.5b02227.

Zhou, Y., Cheng, G., Chen, K., Lu, J., Lei, J., Pu, S., 2019. Adsorptive removal of bisphenol A, chloroxylenol, and carbamazepine from water using a novel β-cyclodextrin polymer. Ecotoxicol. Environ. Saf. 170, 278–285. https://doi.org/10.1016/j.ecoenv.2018.11.117.

Zhou, Y., Hu, Y., Huang, W., Cheng, G., Cui, C., Lu, J., 2018. A novel amphoteric B-cyclodextrin-based adsorbent for simultaneous removal of cationic/anionic dyes and bisphenol A. Chem. Eng. J. 341, 47–57. https://doi.org/10.1016/j.cej.2018.01.155.

Zhou, Yi, He, J., Lu, J., Liu, Y., Zhou, Yanbo, 2020. Enhanced removal of bisphenol A by cyclodextrin in photocatalytic systems: degradation intermediates and toxicity evaluation. Chin. Chem. Lett. 31, 2623–2626. https://doi.org/10.1016/j.cclet.2020.02.008.

Zhou, Z., Guo, Q., Xu, Z., Wang, L., Cui, K., 2015. Distribution and removal of endocrine-disrupting chemicals in industrial wastewater treatment. Environ. Eng. Sci. 32, 203–211. https://doi.org/10.1089/ees.2014.0082.